Eocene Loranthaceae pollen pushes back divergence ages for major splits in the family (#15035)

First revision

Important notes

Declarations

Please read the **Important notes** below, the **Review guidance** on page 2 and our **Standout reviewing tips** on page 3. When ready **submit online**. The manuscript starts on page 4.

Editor Kenneth De Baets	
Files	1 Tracked changes manuscript(s) 1 Rebuttal letter(s) 11 Figure file(s) 5 Table file(s) 8 Raw data file(s) Please visit the overview page to download and review the files not included in this review PDF.

No notable declarations are present



Please read in full before you begin

How to review

When ready <u>submit your review online</u>. The review form is divided into 5 sections. Please consider these when composing your review:

- 1. BASIC REPORTING
- 2. EXPERIMENTAL DESIGN
- 3. VALIDITY OF THE FINDINGS
- 4. General comments
- 5. Confidential notes to the editor
- 1 You can also annotate this PDF and upload it as part of your review

To finish, enter your editorial recommendation (accept, revise or reject) and submit.

BASIC REPORTING

- Clear, unambiguous, professional English language used throughout.
- Intro & background to show context.
 Literature well referenced & relevant.
- Structure conforms to **PeerJ standards**, discipline norm, or improved for clarity.
- Figures are relevant, high quality, well labelled & described.
- Raw data supplied (see **PeerJ policy**).

EXPERIMENTAL DESIGN

- Original primary research within **Scope of** the journal.
- Research question well defined, relevant & meaningful. It is stated how the research fills an identified knowledge gap.
- Rigorous investigation performed to a high technical & ethical standard.
- Methods described with sufficient detail & information to replicate.

VALIDITY OF THE FINDINGS

- Impact and novelty not assessed.
 Negative/inconclusive results accepted.
 Meaningful replication encouraged where rationale & benefit to literature is clearly stated.
- Data is robust, statistically sound, & controlled.
- Conclusions are well stated, linked to original research question & limited to supporting results.
- Speculation is welcome, but should be identified as such.

The above is the editorial criteria summary. To view in full visit https://peerj.com/about/editorial-criteria/

7 Standout reviewing tips



The best reviewers use these techniques

	n
	N

Support criticisms with evidence from the text or from other sources

Give specific suggestions on how to improve the manuscript

Comment on language and grammar issues

Organize by importance of the issues, and number your points

Give specific suggestions on how to improve the manuscript

Please provide constructive criticism, and avoid personal opinions

Comment on strengths (as well as weaknesses) of the manuscript

Example

Smith et al (J of Methodology, 2005, V3, pp 123) have shown that the analysis you use in Lines 241-250 is not the most appropriate for this situation. Please explain why you used this method.

Your introduction needs more detail. I suggest that you improve the description at lines 57-86 to provide more justification for your study (specifically, you should expand upon the knowledge gap being filled).

The English language should be improved to ensure that your international audience can clearly understand your text. I suggest that you have a native English speaking colleague review your manuscript. Some examples where the language could be improved include lines 23, 77, 121, 128 - the current phrasing makes comprehension difficult.

- 1. Your most important issue
- 2. The next most important item
- 3. ...
- 4. The least important points

Line 56: Note that experimental data on sprawling animals needs to be updated. Line 66: Please consider exchanging "modern" with "cursorial".

I thank you for providing the raw data, however your supplemental files need more descriptive metadata identifiers to be useful to future readers. Although your results are compelling, the data analysis should be improved in the following ways: AA, BB, CC

I commend the authors for their extensive data set, compiled over many years of detailed fieldwork. In addition, the manuscript is clearly written in professional, unambiguous language. If there is a weakness, it is in the statistical analysis (as I have noted above) which should be improved upon before Acceptance.



Eocene Loranthaceae pollen pushes back divergence ages for major splits in the family

Friŏgeir Grímsson $^{\text{Corresp.}-1}$, Paschalia Kapli 2 , Christa-Charlotte Hofmann 1 , Reinhard Zetter 1 , Guido W Grimm $^{\text{Corresp.}-1,3}$

Corresponding Authors: Friðgeir Grímsson, Guido W Grimm Email address: fridgeir.grimsson@univie.ac.at, grimmiges@gmail.com

Background: We revisit the palaeopalynological record of Loranthaceae, using pollen ornamentation to discriminate lineages and to test molecular dating estimates for the diversification of major lineages.

Methods: Fossil Loranthaceae pollen from the Eocene and Oligocene are analysed and documented using scanning-electron microscopy. These fossils were associated with molecular-defined clades and used as minimum age constraints for Bayesian node dating using different topological scenarios.

Results: The fossil Loranthaceae pollen document the presence of at least one extant root-parasitic lineage (Nuytsieae) and two currently aerial parasitic lineages (Psittacanthinae and Loranthinae) by the end of the Eocene in the Northern Hemisphere. Phases of increased lineage diversification (late Eocene, middle Miocene) coincide with global warm phases.

Discussion: With the generation of molecular data becoming easier and less expensive every day, neontological research should re-focus on conserved morphologies that can be traced through the fossil record. The pollen, representing the male gametophytic generation of plants and often a taxonomic indicator, can be such a tracer. Analogously, palaeontological research should put more effort into diagnosing Cenozoic fossils with the aim of including them into modern systematic frameworks.

¹ Department of Palaeontology, University of Vienna, Wien, Austria

² The Exelixis Lab, Scientific Computing Group, Heidelberg Institute for Theoretical Studies, Heidelberg, Germany

³ None, Orléans, France





1	Eocene Loranthaceae pollen pushes back divergence ages for major splits in the family
2	Friðgeir Grímsson ¹ , Pashalia Kapli ² , Christa-Charlotte Hofmann ¹ , Reinhard Zetter ¹ , Guido W
3	Grimm ^{1,3}
4	¹ University of Vienna, Department of Palaeontology, Vienna, Austria
5 6 7	 ² The Exelixis Lab, Scientific Computing Group, Heidelberg Institute for Theoretical Studies, Heidelberg, ³ Unaffiliated, Orléans, France
8 9	
10	
11	Corresponding Authors:
12	Althanstraße 14 (UZA II), Vienna, A-1090, Austria
13	Email address: <u>fridgeir.grimsson@univie.ac.at</u>
14	
15	Guido W. Grimm
16	Email address: grimmiges@gmail.com
17	



19 Check author names (species)

20 Abstract [500 words, 3000 characters]

- 21 **Background**: We revisit the palaeopalynological record of Loranthaceae, using pollen
- 22 ornamentation to discriminate lineages and to test molecular dating estimates for the
- 23 diversification of major lineages.
- 24 **Methods:** Fossil Loranthaceae pollen from the Eocene and Oligocene are analysed and
- documented using scanning-electron microscopy. These fossils were associated with molecular-
- 26 defined clades and used as minimum age constraints for Bayesian node dating using different
- 27 topological scenarios.
- 28 **Results:** The fossil Loranthaceae pollen document the presence of at least one extant root-
- 29 parasitic lineage (Nuytsieae) and two currently aerial parasitic lineages (Psittacanthinae and
- 30 Loranthinae) by the end of the Eocene in the Northern Hemisphere. Phases of increased lineage
- 31 diversification (late Eocene, middle Miocene) coincide with global warm phases.
- 32 **Discussion:** With the generation of molecular data becoming easier and less expensive every
- day, neontological research should re-focus on conserved morphologies that can be traced
- 34 through the fossil record. The pollen, representing the male gametophytic generation of plants
- and often a taxonomic indicator, can be such a tracer. Analogously, palaeontological research
- 36 should put more effort into diagnosing Cenozoic fossils with the aim of including them into
- 37 modern systematic frameworks.

Introduction

38

- The Loranthaceae (order Santalales), a moderately large family comprising about 76 genera
- and over 1000 species in five tribes (Nickrent 1997 onwards; Nickrent et al. 2010), has a wide
- 41 geographical distribution. Today, there is a relatively clear geographic split between a New
- 42 World group (Psittacanthinae) and Old World-Australasian lineages (Elythrantheae and
- 43 Lorantheae), which gave rise to the hypothesis that the initial Loranthaceae diversification was
- linked to the final phase of the Gondwana breakup in the Late Cretaceous (e.g. Barlow 1990;
- 45 Vidal-Russell & Nickrent 2007). Only three of the more than 70 genera are root parasites and the
- 46 rest are aerial branch parasites. Molecular studies on Loranthaceae (and Santalales in general)



- 47 have thus focused on three issues: 1) clarifying the evolutionary relationships within the family
- 48 (Vidal-Russell & Nickrent 2008a); 2) explaining the transition from root to aerial parasitism
- 49 (Wilson & Calvin 2006); 3) dating the time of transition to aerial parasitism (Vidal-Russell &
- Nickrent 2008b). All molecular studies using outgroups recognised the south-western Australian,
- 51 root-parasitic, monotypic Nuytsia R.Br. (monogeneric tribe Nuytsieae; Nickrent et al. 2010) as
- 52 the first diverging lineage in the family (Wilson & Calvin 2006; Vidal-Russell & Nickrent
- 53 2008a; Su et al. 2015). The other two Loranthaceae root parasites (Atkinsonia F.Muell.,
- 54 Gaiadendron G.Don; tribe Gaiadendreae) formed a grade to the New World aerial parasites
- 55 (Wilson & Calvin 2006; multiple origins of aerial parasitism) or all aerial parasitic genera of the
- 56 family (Vidal-Russell & Nickrent 2008a; Vidal-Russell & Nickrent 2008b; Su et al. 2015;
- 57 singular origin). Using a time-calibrated phylogeny, Vidal-Russell and Nickrent (2008b)
- 58 concluded that Loranthaceae diverged from other Santalales lineages in the uppermost
- 59 Cretaceous. The first radiation the divergence of root parasites *Nuytsia*, *Atkinsonia* and
- 60 Gaiadendron was during the Eocene. The crown age of the aerial parasitic clade within the
- 61 Loranthaceae, comprising the mostly New World Psittacantheae and Old World-Australasian
- 62 Erytrantheae and Lorantheae, was placed in the middle Oligocene, approximately 28 Ma
- 63 (estimated via a Bayesian relaxed clock and fixing the Santalales root to a maximum age of 114
- 64 Ma); a time characterised by global cooling (Zachos et al. 2001) and retreat of subtropical and
- 65 tropical vegetation.
- Although molecular and morphological interrelationships of Loranthaceae genera are
- 67 considered now to be relatively clear (Nickrent et al. 2010; Su et al. 2015; but see Grímsson,
- 68 Grimm & Zetter 2017), the timing of divergence between the genera has not been cross-checked
- 69 with available evidence from the fossil record (e.g. Muller 1981; Song, Wang & Huang 2004;
- Macphail et al. 2012). Also, the phytogeographic history of the family is based merely on the
- 71 present distribution of its genera (e.g. Vidal-Russell & Nickrent 2007) and has not yet been
- 72 explored in detail (Vidal-Russell & Nickrent 2008a: p. 1027). The latest hypothesis put forward
- vas that Loranthaceae originated when South America, Antarctica and Australia were still
- 74 connected, and that two large-scale migration events, one from New Zealand and one from
- Australia, shaped the modern distribution (Vidal-Russell & Nickrent 2008a, 2008b). The single
- shift to aerial parasitism was estimated to be of middle Oligocene age. Thus, older fossil records,



104

78 root parasites or extinct clades of aerial parasites (Macphail et al. 2012). 79 The outstanding work on the pollen morphology of extant Loranthaceae by Feuer & Kuijt 80 (1979, 1980, 1985) and other Santalales lineages (Maguire, Wurdack & Huang 1974; Feuer 81 1977; Feuer 1978; Feuer & Kuijt 1978; Feuer 1981; Feuer & Kuijt 1982; Feuer, Kuijt & Wiens 82 1982) demonstrated that most pollen produced by members of the Loranthaceae cannot be 83 confused with pollen from other angiosperm families (Grímsson, Grimm & Zetter 2017). 84 Grímsson, Grimm & Zetter (2017) distinguished four general types (Pollen Type A, B, C, D), of 85 which only one (Pollen Type A) could be confused with pollen of other Santalales lineages, and 86 would unlikely be recognised as Loranthaceae pollen if found in a fossil pollen sample. 87 Combined application of light microscopy (LM), scanning-electron microscopy (SEM), and 88 transmission electron microscopy (TEM) revealed that pollen morphologies – including the 89 many variants of B-type pollen – are conserved at various taxonomic levels within Loranthaceae 90 (Feuer & Kuijt 1978; Feuer & Kuijt 1979; Feuer & Kuijt 1980; Feuer & Kuijt 1985; Caires 2012; 91 Grímsson, Grimm & Zetter 2017). Thus, dispersed fossil pollen can aid in the reconstruction of 92 past distributions of Loranthaceae lineages and shed light on the timing of the origin of the 93 modern clades. Being the male gametophyte of a plant, pollen are generally conserved in 94 morphology. Diagnostic (lineage-specific) pollen hence allow for the tracing of modern lineages 95 deep into the past (e.g. Zetter, Hesse & Huber 2002; Grímsson, Zetter & Hofmann 2011; 96 Grímsson et al. 2016). 97 Here, we describe new fossil Loranthaceae pollen grains from the middle Eocene of the 98 United States, Greenland, Central Europe, and East Asia, and from the late Oligocene/early 99 Miocene of Germany. The diagnostic morphological features of the pollen provided sufficient 100 details to assign the fossil pollen to distinct lineages within the Loranthaceae. These fossil pollen represent the earliest unambiguous reports of the root parasitic Nuytsieae, and the presently 101 102 aerial parasitic lineages Psittacanthinae, Elytrantheae and Lorantheae. Thus, they can be used as 103 potential ingroup minimum age priors for node dating, and to refine our knowledge about the

the oldest going back to the early Eocene (c. 50 Ma) in Australia, were considered to represent

evolutionary history of the Loranthaceae.



Material & Methods

106	Origin of samples and geological background (Table 1)
107	The fossil Loranthaceae pollen identified during this study occurred in six different sediment
108	samples: (1) the Claiborne Group of the Miller Clay Pit in Henry County, Tennessee, United
109	States (sample UF 15817-062117); (2) the Hareøen Formation (middle Eocene) on
110	Qeqertarsuatsiaq Island (Hareøen), western Greenland; (3) the Borkener coal measures of the
111	Stolzenbach underground coal mine, near Kassel, Germany; (4) the Profen Formation (middle
112	Eocene) of the Profen opencast mine, close to Leipzig in Germany; (5) the Changchang
113	Formation (middle Eocene) on northern Hainan Island, South China; (6) the Melker Series of the
114	NÖ05 borehole positioned close to Theiss, near Krems, Lower Austria; and (7) the
115	Cottbus/Spremberg Formations (late Oligocene/early Miocene) of Altmittweida in Saxony,
116	Germany. For details on the geographic positions, geology, paleoecology, and previously known
117	fossil plants from these formations and localities see Table 1 and references therein. Epoch
118	names and ages in Table 1 follow Cohen et al. (2013 [updated]).
119	Preparation of samples
120	The sedimentary rock samples were processed according to the protocols outlined in
121	Grímsson, Denk & Zetter (2008). We investigated the fossil Loranthaceae pollen grains using the
122	'single grain method' (Zetter 1989), whereby the same fossil pollen grain is first analysed under
123	the LM and then SEM. SEM stubs produced under this study are stored in the collection of the
124	Department of Palaeontology, University of Vienna, Austria, under accession numbers IPUW
125	7513/076-100.
126	Molecular framework (File S1: Steps 1-3 of analysis pipeline)
127	For molecular data, we relied on a 2014 NCBI GenBank harvest compiled for an earlier study
128	(Grímsson, Grimm & Zetter 2017). Gene banks now (as of Dec 1st, 2016) include ~100
129	additional accessions (File S2); but the majority of these are either microsatellite marker
130	sequences or sequences of gene regions too variable, or with insufficient taxonomic coverage
131	within the Loranthaceae, to be of any use; thus, we opted against updating the dataset harvested



132	for the preceding study. All analysis files (sorted by steps) are included in the online supporting
133	archive (OSA) in the Supplementary Information.
134	Given the problems with signals in Loranthaceae sequence data (Grímsson, Grimm & Zetter
135	2017, files S1, S6), we used the following protocol to prepare data sets for phylogenetic
136	inferences and molecular dating (a detailed description is provided in File S1). First, we
137	performed single-gene maximum likelihood (ML) inferences for five candidate gene regions
138	using the complete harvested data with RAxML v. 8.2.4 (Stamatakis 2014). This was mainly
139	done to cross-check for problematic accessions and to test the phylogenetic coherence of
140	multiple accessions of the same species/genus. As a consequence, we eliminated several more
141	sequences, in addition to the ones not considered earlier, for computing strict genus-consensus
142	sequences (see File S1, an emended version of Grímsson, Grimm & Zetter 2017, file S2). The
143	second step was to consense and concatenate the unproblematic data: strict species-consensus
144	sequences, i.e. sequences summarising the information of accessions attributed to a species, were
145	computed with G2CEF (Göker & Grimm 2008) and concatenated with MESQUITE v. 2.75
146	(Maddison & Maddison 2011). The third and final step was the inference of single- and oligo-
147	gene ML trees using RAxML v. 8.2.4; branch support was established using non-parametric
148	bootstrapping with the number of necessary bootstrap replicates determined by the extended
149	majority rule consensus bootstop criterion (Pattengale et al. 2009). Potentially conflicting signals
150	were explored using bootstrap (BS) consensus networks (bipartition networks; Grimm et al.
151	2006), a special form of consensus networks (Holland & Moulton 2003) generated with
152	SPLITSTREE v. 14.2 (option "count", Huson & Bryant 2006) in which edge lengths are
153	proportional to the frequency of the according split in the BS (pseudo)replicate sample. The
154	complex signal and overall divergence in the molecular data calls for a probabilistic inference
155	method (i.e. ML or Bayesian inference), and a means for establishing branch support that can
156	reflect the robustness of (partly) conflicting signals from the data. Regarding the latter, non-
157	parametric bootstrapping (BS) is more informative (conservative) than Bayesian-inferred
158	posterior probabilities (PP). If a certain proportion of alignment patterns (e.g. 30%) support a
159	split B that is in conflict with the dominant split A (supported by 70% of the alignment patterns),
160	the BS support under ML (BS $_{ML})$ will be accordingly split in the optimal case (BS $_{ML}\!\sim\!70$ for A
161	vs. $BS_{ML} \sim 30$ for B). The PP may converge to 1 for A and 0 for B as the MCMC chain(s)
162	optimise(s) towards the topology that best explains the complete data. For the example of



Loranthaceae, it can be demonstrated that branches with $PP \sim 1 \gg BS_{ML}$ in the tree of Su et al. (2015) relate to relationships supported only by one gene region (matK), which outcompetes conflicting, partly unambiguous signals from all other gene regions; the latter captured in the BS pseudoreplicate samples (Grímsson, Grimm & Zetter 2017, file S6). Readers interested in the behaviour of PP in comparison to the BS_{ML} support values used here can find the according information in the Supporting Information (File S1: set-up, File S5: results; Bayesian sampled topology files are included in the OSA).

Clock-rooting (Table 2; Step 4 of analysis pipeline)

171	A recent re-analysis of available molecular data using genus-consensus sequences (Grímsson,
172	Grimm & Zetter 2017) failed to unambiguously resolve basal relationships in Loranthaceae as
173	was the case in earlier studies using placeholder accessions (Wilson & Calvin 2006; Vidal-
174	Russell & Nickrent 2008a; Su et al. 2015; see Grímsson, Grimm & Zetter 2017, file S6, for a
175	critical assessment of the Loranthaceae data included by Su et al.). The problem of topological
176	ambiguity worsens for the species tree inferred here, in part due to data gaps (see Inferences and
177	supplement to Grímsson, Grimm & Zetter, 2017). Due to issues regarding ambiguity of the
178	deepest splits within the Loranthaceae and likely outgroup-ingroup long-branch attraction
179	(Grímsson, Grimm & Zetter 2017, file S6), we inferred an alternative, clock-based root
180	(Huelsenbeck, Bollback & Levine 2002) for the Loranthaceae tree using BEAST v. 1.8.2
181	(Drummond & Rambaut 2007; Drummond et al. 2012), following the example of an earlier study
182	on Acer (Renner et al. 2008). Clock-rooting was performed for five main datasets differing in the
183	gene region coverage (all gene regions, all but excluding the most variable trnL-trnF spacer
184	region, only plastid regions including or excluding the trnL-trnF spacer, only nuclear regions). In
185	addition, the taxon-reduced data set used for the final dating step was analysed (for further
186	details see File S1). For each of the matrices we performed a BEAST run under partition specific
187	substitution models, unconstrained tree topology, a Yule tree prior, and uncorrelated log-normal
188	clock prior [ucld.mean \sim Gamma (0.001, 1000)]. The best fitting substitution models per
189	partition, among the available in BEAST, were selected with JMODELTEST (Darriba et al. 2012).
190	Each analysis was conducted for 2*10 ⁷ generations with a sampling frequency of 10 ⁻³ (for further
191	details see File S1).



Basic setup of molecular dating (Table 2; Steps 5 and 6 of analysis pipeline) 192 Nine of the 13 new described fossil pollen from the Eocene to Oligocene (see **Results**) were 193 194 used as minimum age constraints (informing 3–5 node height priors per analysis) for traditional 195 node dating using a Bayesian uncorrelated clock (UC) approach; analyses were performed with 196 BEAST v. 1.8.2. Table 2 lists the age priors used for the analyses. Dating was done in two phases (for set-up details see File S1). With respect to the non-trivial matrix signals and the branch-197 lengths seen in the ML tree, rate shifts should be considered during dating. Hence, we chose to 198 199 use the UC approach over other node-dating alternatives (e.g. Renner et al. 2008; Smith, 200 Beaulieu & Donoghue 2009; see e.g. Dornburg et al. 2012 for bias in the case of mammal 201 mtDNA). 202 In the initial phase (Step 5), we inferred dated species phylogenies based on the complete 203 concatenated data set for three rooting scenarios: (i) the commonly accepted root placing Nuytsia 204 as sister to all other Loranthaceae (Vidal-Russell & Nickrent 2008a; Nickrent et al. 2010; Su et 205 al. 2015); (ii) a clock-inferred root recognising the predominately Old World Lorantheae as sister 206 to a mainly southern hemispheric clade that includes all three root parasites, the Psittancantheae 207 and Elytrantheae (see *Results*); and (iii) recognising *Tupeia* as sister to all other Loranthaceae. The 3^{rd} scenario is based on the hypothesis that the typical oblate, \pm triangular Loranthaceae 208 209 pollen (Pollen Type B in Grímsson, Grimm & Zetter 2017, a pollen type unique within the 210 Santalales) evolved only once. The monotypic *Tupeia* is one of two Loranthaceae species with a 211 spheroidal, echinate pollen as found in other Santalales lineages (Grímsson, Grimm & Zetter 212 2017) and the only one sequenced so far. Irrespective of the data used, *Tupeia* is the taxon with 213 the smallest root-tip distance within Loranthaceae, including trees rooted with *Nuvtsia* (Su et al. 214 2015, fig. 1B; Grímsson, Grimm & Zetter 2017; this study). 215 For the final dating (Step 6), we used a taxon-reduced data set limited to 42 species covering 216 all included gene regions to counter problems with missing data in the full data set. At this step 217 we also included an alternative topology, which constrained the primary branching patterns seen 218 in the tree of Su et al. (2015). This alternative topology was suggested by an anonymous 219 reviewer reporting on the draft to Grímsson, Grimm & Zetter (2017) to depict the correct 220 relationships between the major lineages and potentially early diverging, isolated, monotypic genera. Each analysis ran for 5*10⁷ MCMC steps, under a similar set-up as described in the 221 222 preceding step (*Clock-rooting*). The tree was partially constrained each time to accommodate the



PeerJ

223	placement of the fossils and the corresponding rooting hypothesis (see xml-setup files provided
224	in the online supporting material, OSM, for details). Each analysis was run twice to ensure the
225	runs converged to the stationary distribution. Finally, all age calibration priors (Table S1-1 in
226	File S1) were modelled as normal distributions around the midpoint of the known time intervals
227	(for further details see File S1). With respect to the variations in plant evolutionary rates (e.g.
228	Guzmán & Vargas 2010; Lockwood et al. 2013), we opted against performing any rate-based
229	dating. Smith & Donoghue (2008) cautioned against the use of rate-based estimates of
230	divergence times even when fossil calibration priors are lacking as it may lead to strong biases.

Descriptions (Figs 1–6)

Some lineages (tribes, subtribes) and genera of modern Loranthaceae are characterised by



251	Miller Clay Pit MT1, aff. Nuytsia (Figs 1A, 1B, 2A, SH; Plate S01, S02 in File
252	<i>S3)</i>
253	Description—Pollen, oblate, concave triangular in polar view, no undistorted equatorial view
254	available, equatorial apices obcordate, interapertural areas (mesocolpia) sunken; pollen small,
255	equatorial diameter 15.0–18.3 μm in LM, 13.0–14.4 μm in SEM; zono(3)colpate, colpi long and
256	narrow; exine 0.7-0.8 µm thick, nexine thinner than sexine; tectate; sculpturing psilate in LM,
257	microechinate in area of mesocolpium in SEM, echini 0.3-0.8 μm long, 0.2-0.5 μm wide at base
258	(SEM); margo well developed, broad, psilate to partly granulate (SEM); colpus membrane not
259	observed.
260	Locality—Miller Clay Pit, Henry County, Tennessee, United States (Table 1).
261	Remarks—This pollen type is very similar to pollen of the extant southwestern Australian
262	Nuytsia floribunda (Labill.) G.Don as figured by Feuer & Kuijt (1980) and Grímsson, Grimm &
263	Zetter (2017); a pollen readily distinct from all other modern Loranthaceae. The fossil pollen
264	only differs from Nuytsia by being zonocolpate and showing sunken (infolded) mesocolpia in
265	LM and SEM. The shift from the basic syncolpate organisation to zonocolpate can be observed
266	in several lineages of (modern) Loranthaceae. With respect to the high genetic distinctness of
267	Nuytsia from all other Loranthaceae, the modern species likely represents the sole survivor of an
268	early diverged lineage of root parasitic loranths. Hence, it is likely that ancestral or extinct
269	members of Nuytsia/Nuytsieae had more morphological variation than can be observed in the
270	sole surviving species.
271	Use as age constraint—The Miller Clay Pit MT1 can be used to constrain the root age of the
272	lineage leading to Nuytsia, i.e. the Nuytsieae root age. Based on the currently available molecular
273	data, the relationship of Nuytsia to the remainder of the genus and the other two extant root
274	parasites is unclear. Nevertheless, Nuytsia is likely the sole modern-day representative of an
275	early diverging lineage. For rooting scenario 1 (outgroup-inferred root) Miller Clay Pit MT1
276	serves as minimum age constraint for the MRCA of all (extant) Loranthaceae.
277	
278	Miller Clay Pit MT2, aff. Tripodanthus (Figs 1C, 3A, 3G; Plate S03 in File S3)
279	Description—Pollen, oblate, concave-triangular in polar view, no undistorted equatorial view
280	available, equatorial apices T-shaped; pollen small, equatorial diameter 18.3–21.7 µm in LM,

PeerJ

- 281 17.9–20.2 μm in SEM; syn(3)colpate, colpi narrow; exine 1.2–1.5 μm thick, nexine thinner than
- sexine, intercolpial nexine thickening at pole, sexine thickened in area of mesocolpium (LM);
- 283 tectate; sculpturing psilate in LM, (micro)baculate in area of mesocolpium in SEM,
- 284 (micro)bacula densely packet, 0.2–0.9 µm long, 0.2–0.4 µm wide (SEM); margo well-developed,
- 285 widening towards pole and equator, mostly psilate, with few nanoechini/-verrucae (SEM); colpus
- 286 membrane not observed.
- 287 Locality—Miller Clay Pit, Henry County, Tennessee, United States (Table 1).
- 288 Remarks—Pollen grains of this morphotype show the exclusive morphology of pollen of two
- of the three extant *Tripodanthus* species: *T. acutifolius* (Ruiz & Pav.) Tiegh. and *T. flagellaris*
- 290 Tiegh. as described and figured by Feuer & Kuijt (1980) and Grímsson, Grimm & Zetter (2017).
- 291 The recently described T. belmirensis F.J.Roldán & Kuijt has a different, more compact type of
- 292 pollen (Roldán & Kuijt 2005). All species are endemic to South America (e.g., Amico et al.
- 293 2012).
- 294 Use as age constraint—Representing a characteristic pollen type known only from two
- 295 modern species of the same genus, Miller Clay Pit MT2, MT3, and the Aamaruutissaa MT could
- be used as minimum age constraints for the MRCA of *Tripodanthus* with respect to T.
- 297 belmirensis and its different pollen. We followed a more conservative approach here.
- 298 *Tripodanthus* is often reconstructed as the first diverging branch within the Psittacanthinae,
- 299 followed in most trees by *Psittacanthus*. The latter is a genus with diverse pollen (Feuer & Kuijt
- 300 1979), including morphologies more similar to those of *Tripodanthus* and its fossil counterparts
- than to the remainder of the subtribe (and *T. belmirensis*). The remainder is characterised by
- 302 compact B-type pollen with minute to indistinct sculpturing and pollen grains of the Type C
- 303 (Passovia pyrifolia, Dendropemon) and D (Oryctanthus). Compact B-type, C-type and D-type
- pollen occur much later in the fossil record (File S4) and are completely missing in our samples.
- 305 The latter three types appear to be derived. Taking all evidence into account, we cannot exclude
- 306 the possibility that *Tripodanthus acutifolius* and *T. flagellaris* simply retained a more ancestral
- 307 pollen type of the Psittacanthinae. The fossil pollen grains hence would not indicate the presence
- 308 of the genus *Tripodanthus* in North America and Greenland, but of extinct, northern-hemispheric
- or ancestral members of the Psittacanthinae, thereby informing a conservative minimum age for
- 310 the MRCA of Psittacanthinae and their sister clade. Unfortunately, this sister clade, if not
- 311 constrained (scenario 4), is not resolved with meaningful support. As a trade-off, we used the



312	Aamaruutissaa MT – the most precisely dated pollen of the <i>Tripodanthus</i> -like MTs and likely
313	younger than their American counterparts – as minimum age constraint for the MRCA of the
314	Psittacanthinae lineage for the rooting scenarios 1-3 (under the assumption that crown radiation
315	within the Psittacanthinae must have started before the time of a loranth that produced
316	Tripodanthus-like pollen and thrived in Greenland, far outside the modern distribution area of
317	the family.)
318	
319	Miller Clay Pit MT3, aff. Tripodanthus (Figs 1D, 3B, 3C, 3H, 3I; Plate S04 in
320	File S3)
321	Description—Pollen, oblate, slightly concave-triangular in polar view, no undistorted
322	equatorial view available, equatorial apices truncated; pollen small, equatorial diameter 20.0-
323	$21.7~\mu m$ in LM, 19.6 – $21.3~\mu m$ in SEM; syn(3)colpate, colpi narrow; exine 0.9 – $1.6~\mu m$ thick,
324	nexine thinner than sexine, intercolpial nexine thickening at pole, sexine thickened in area of
325	mesocolpium (LM); tectate; sculpturing psilate in LM, (micro)baculate and perforate in area of
326	mesocolpium in SEM, (micro)bacula densely packet, (micro)bacula 0.4–1.8 µm long, 0.1–0.2
327	μm wide; margo well developed, markedly broader in equatorial regions, margo faintly nano- to
328	microrugulate (SEM); colpus membrane nanoverrucate to granulate (SEM).
329	Locality—Miller Clay Pit, Henry County, Tennessee, United States (Table 1).
330	Remarks—General outline and size of the Miller Clay Pit MT3 is very similar to those of
331	Miller Clay Pit MT2. The main difference is that the margo in Miller Clay Pit MT3 can be
332	faintly rugulate, a feature not observed in Miller Clay Pit MT2 or the two extant species with
333	nearly identical pollen. Also, the mesocolpium is perforate in Miller Clay Pit MT3; a feature no
334	seen in Miller Clay Pit MT2 or extant <i>Tripodanthus</i> . As a trend, the sculptural elements are
335	narrower and can be much longer than in Miller Clay Pit MT2 pollen.
336	Use as age constraint—See Miller Clay Pit MT2.
337	Aamaruutissaa MT, aff. Tripodanthus (Figs 1E, 3D, 3J; Plate S05 in File S3)
338	Description—Pollen, oblate, slightly concave-triangular in polar view, no undistorted
339	equatorial view available, equatorial apices truncated; pollen small, equatorial diameter 18.6-
340	22.0 μm in LM, 18.5–21.5 μm in SEM; syn(3)colpate; exine 1.0–1.3 μm thick, nexine thinner



341	than sexine, intercolpial nexine thickening at pole (LM); tectate; sculpturing psilate in LM, nano
342	to microbaculate in area of mesocolpium in SEM, bacula $0.3-1.1~\mu m$ long, $0.2-0.3~\mu m$ wide
343	(SEM); margo well developed, margo faintly nano- to microrugulate (SEM); colpus membrane
344	nanoverrucate to granulate (SEM).
345	Locality—Aamaruutissaa, southeast Qeqertarsuatsiaq Island, western Greenland (Table 1).
346	Remarks—This pollen type has previously been figured as Loranthaceae gen. et spec. indet.
347	(Manchester, Grímsson & Zetter 2015, fig. 2A-C). Like Miller Clay Pit MT2 and MT3, it is
348	nearly indistinguishable from the pollen of the two original species of Tripodanthus, T.
349	acutifolius and T. flagellaris. The Aamaruutissaa MT pollen combines the mesocolpial
350	sculpturing seen in Miller Clay Pit MT2 with the shape and margo seen in Miller Clay Pit MT3.
351	With respect to the modern species, both the Tennessee (Miller Clay Pit MT2, MT3) and
352	Greenland pollen grains (Aamaruutissaa MT) were possibly produced by the same genus or at
353	least closely related taxa of the same loranth lineage (Psittacanthinae).
354	Use as age constraint—See Miller Clay Pit MT2.
355	Stoleonback MT mollon of ambiguous affinity (Figs 15, 28, 21; Blata 506 in
	Stolzenbach MT, pollen of ambiguous affinity (Figs 1F, 2B, 2I; Plate S06 in
356	File S3)
357	Description—Pollen, oblate, trilobate in polar view, no undistorted equatorial view available,
358	equatorial apices obcordate, interapertural areas (mesocolpia) sunken; pollen small, equatorial
359	diameter 12.1–15.4 μm in LM, 11.7–15.3 μm in SEM; syn(3)colpate, colpi narrow; exine 0.7–
360	0.9 μm thick, nexine thinner than sexine; tectate; sculpturing psilate in LM, microechinate in
861	area of mesocolpium in SEM, echini stout with blunt apices, 0.4–0.8 μm long, 0.3–0.8 μm wide
362	at base (SEM); margo well developed, broad, covering the grain's surface in polar view,
363	microrugulate, granulate (SEM); colpus membrane mostly granulate (SEM).
364	Locality—Stolzenbach underground coalmine, Kassel, Germany (Table 1).
365	Remarks—Size, outline, and form of the pollen, and SEM sculpturing in the area of the
366	mesocolpium is most similar to what has been observed in pollen of modern monotypic root-
367	parasites Nuytsia and Gaiadendron, and the Lorantheae Muellerina (Ileostylinae). Despite this
368	general similarity, the pollen differs from the modern ones and pollen with affinity to Nuytsia
369	reported from the Miller Clay Pit, Tennessee (Miller Clay Pit MT1), visually (compare
370	overviews in Fig. 2B, E, F, G) and regarding its sculpturing. The Stolzenbach MT echini are



371	sparsely packed and broader at the base; the striae on the margo are flatter and broader. The
372	pollen may well represent an unrelated, extinct lineage or ancestral taxon with affinities to both
373	the root-parasitic lineages and/or the Lorantheae.
374	Use as age constraint—Although the pollen cannot be assigned to any modern genus or
375	lineage, it is an early Central European representative of the common Pollen Type B of
376	Loranthaceae. Its morphology is in many aspects primitive within the (B-type) Loranthaceae,
377	hence, the similarity with Nuytsia/Miller Clay Pit MT1, Gaiadendron and Muellerina (the only
378	Lorantheae known so far with a striate ornamentation). Its morphology, place, and age would fit
379	for an early precursor or extinct sister lineage of the Lorantheae. Taken together with the coeval
380	pollen from North America and Greenland, it provides evidence for the onset of diversification
381	of B-type pollen lineages including the possible establishment of the Lorantheae. Hence, it was
382	used to constrain the minimum age of the MRCA of all Loranthaceae (rooting scenario 2; clock-
383	based root) or Loranthaceae with B-type pollen (rooting scenario 3; pollen morphology-informed
384	root).
205	
385	
	Duefon MT1 mollon of unknown offinity (Fine 1C 1U 2C 21 Dieto CO7 in File
386	Profen MT1, pollen of unknown affinity (Figs 1G, 1H, 2C, 2J; Plate S07 in File
386 387	<i>53)</i>
386 387 388	<i>Description</i> —Pollen, oblate, trilobate in polar view, elliptic in equatorial view, lobes very
386 387 388 389	Description—Pollen, oblate, trilobate in polar view, elliptic in equatorial view, lobes very narrow, equatorial apices obcordate, interapertural areas (mesocolpia) sunken; pollen small,
386 387 388	Description—Pollen, oblate, trilobate in polar view, elliptic in equatorial view, lobes very narrow, equatorial apices obcordate, interapertural areas (mesocolpia) sunken; pollen small, polar axis 10.0-12.3 μm long in LM, 9.5–11.0 μm long in SEM, equatorial diameter 13.8–17.5
386 387 388 389	Description—Pollen, oblate, trilobate in polar view, elliptic in equatorial view, lobes very narrow, equatorial apices obcordate, interapertural areas (mesocolpia) sunken; pollen small,
386 387 388 389 390	Description—Pollen, oblate, trilobate in polar view, elliptic in equatorial view, lobes very narrow, equatorial apices obcordate, interapertural areas (mesocolpia) sunken; pollen small, polar axis 10.0-12.3 μm long in LM, 9.5–11.0 μm long in SEM, equatorial diameter 13.8–17.5
386 387 388 389 390 391	Description—Pollen, oblate, trilobate in polar view, elliptic in equatorial view, lobes very narrow, equatorial apices obcordate, interapertural areas (mesocolpia) sunken; pollen small, polar axis 10.0-12.3 μm long in LM, 9.5–11.0 μm long in SEM, equatorial diameter 13.8–17.5 μm in LM, 11.9–13.8 μm in SEM; syn(3)colpate; exine 0.9–1.1 μm thick, nexine thinner than
386 387 388 389 390 391 392	Description—Pollen, oblate, trilobate in polar view, elliptic in equatorial view, lobes very narrow, equatorial apices obcordate, interapertural areas (mesocolpia) sunken; pollen small, polar axis 10.0-12.3 μm long in LM, 9.5–11.0 μm long in SEM, equatorial diameter 13.8–17.5 μm in LM, 11.9–13.8 μm in SEM; syn(3)colpate; exine 0.9–1.1 μm thick, nexine thinner than sexine; tectate; sculpturing psilate in LM, nanoechinate, nanobaculate, granulate in area of
386 387 388 389 390 391 392 393	Description—Pollen, oblate, trilobate in polar view, elliptic in equatorial view, lobes very narrow, equatorial apices obcordate, interapertural areas (mesocolpia) sunken; pollen small, polar axis 10.0-12.3 μm long in LM, 9.5–11.0 μm long in SEM, equatorial diameter 13.8–17.5 μm in LM, 11.9–13.8 μm in SEM; syn(3)colpate; exine 0.9–1.1 μm thick, nexine thinner than sexine; tectate; sculpturing psilate in LM, nanoechinate, nanobaculate, granulate in area of mesocolpium in SEM, echini/bacula 0.3–0.6 mm long, 0.2–0.4 μm wide (SEM); margo well-
386 387 388 389 390 391 392 393 394	Description—Pollen, oblate, trilobate in polar view, elliptic in equatorial view, lobes very narrow, equatorial apices obcordate, interapertural areas (mesocolpia) sunken; pollen small, polar axis 10.0-12.3 μm long in LM, 9.5–11.0 μm long in SEM, equatorial diameter 13.8–17.5 μm in LM, 11.9–13.8 μm in SEM; syn(3)colpate; exine 0.9–1.1 μm thick, nexine thinner than sexine; tectate; sculpturing psilate in LM, nanoechinate, nanobaculate, granulate in area of mesocolpium in SEM, echini/bacula 0.3–0.6 mm long, 0.2–0.4 μm wide (SEM); margo well-developed, covering nearly the entire surface of the grain in polar view, faintly microrugulate
386 387 388 389 390 391 392 393 394 395	Description—Pollen, oblate, trilobate in polar view, elliptic in equatorial view, lobes very narrow, equatorial apices obcordate, interapertural areas (mesocolpia) sunken; pollen small, polar axis 10.0-12.3 μm long in LM, 9.5–11.0 μm long in SEM, equatorial diameter 13.8–17.5 μm in LM, 11.9–13.8 μm in SEM; syn(3)colpate; exine 0.9–1.1 μm thick, nexine thinner than sexine; tectate; sculpturing psilate in LM, nanoechinate, nanobaculate, granulate in area of mesocolpium in SEM, echini/bacula 0.3–0.6 mm long, 0.2–0.4 μm wide (SEM); margo well-developed, covering nearly the entire surface of the grain in polar view, faintly microrugulate (SEM); colpus membrane nanoverrucate to granulate (SEM).
386 387 388 389 390 391 392 393 394 395 396	Description—Pollen, oblate, trilobate in polar view, elliptic in equatorial view, lobes very narrow, equatorial apices obcordate, interapertural areas (mesocolpia) sunken; pollen small, polar axis 10.0-12.3 μm long in LM, 9.5–11.0 μm long in SEM, equatorial diameter 13.8–17.5 μm in LM, 11.9–13.8 μm in SEM; syn(3)colpate; exine 0.9–1.1 μm thick, nexine thinner than sexine; tectate; sculpturing psilate in LM, nanoechinate, nanobaculate, granulate in area of mesocolpium in SEM, echini/bacula 0.3–0.6 mm long, 0.2–0.4 μm wide (SEM); margo well-developed, covering nearly the entire surface of the grain in polar view, faintly microrugulate (SEM); colpus membrane nanoverrucate to granulate (SEM). Locality—Profen, Leipzig, Central Germany (Table 1).
386 387 388 389 390 391 392 393 394 395 396 397	Description—Pollen, oblate, trilobate in polar view, elliptic in equatorial view, lobes very narrow, equatorial apices obcordate, interapertural areas (mesocolpia) sunken; pollen small, polar axis 10.0-12.3 μm long in LM, 9.5–11.0 μm long in SEM, equatorial diameter 13.8–17.5 μm in LM, 11.9–13.8 μm in SEM; syn(3)colpate; exine 0.9–1.1 μm thick, nexine thinner than sexine; tectate; sculpturing psilate in LM, nanoechinate, nanobaculate, granulate in area of mesocolpium in SEM, echini/bacula 0.3–0.6 mm long, 0.2–0.4 μm wide (SEM); margo well-developed, covering nearly the entire surface of the grain in polar view, faintly microrugulate (SEM); colpus membrane nanoverrucate to granulate (SEM). Locality—Profen, Leipzig, Central Germany (Table 1). Remarks—Like the Stolzenbach MT pollen this fossil pollen type has no direct modern



+01	grains are only known from the foot-parasites <i>wuyisia</i> and <i>Gaidaenaron</i> , and the Lorantheae
402	Muellerina. Equally minute sculpturing is only found in otherwise completely different, and
403	putatively derived pollen of deeply nested (phylogenetically) Psittacanthinae and Lorantheae.
404	Use as age constraint—Showing a unique combination of putatively primitive and derived
405	morphological features, this pollen could only be used to constrain the minimum age of the
406	MRCA of all Loranthaceae with B-type pollen.
407	
408	Profen MT2, aff. Notanthera (Figs 1I, 1J, 4A, 4B, 5A, 5B; Plate S08 in File S3)
109	Description-Pollen, oblate, straight- to slightly concave-triangular in polar view, no
410	undistorted equatorial view available, equatorial apices obcordate; pollen small, equatorial
411	diameter 21.5-23.1 μm in LM, 18.3-19.6 μm in SEM; syn(3)colpate, colpi narrow; exine 1.1-
412	1.4 µm thick, nexine thinner than sexine, intercolpial nexine thickening at pole, sexine thickened
413	in area of mesocolpium (LM); tectate; sculpturing psilate in LM, nanoechinate/-baculate,
414	perforate in area of mesocolpium in SEM, echini/bacula stout, sometimes fused, $0.20.4~\mu m$
415	long, 0.2-0.4 µm wide (SEM); margo well-developed, slightly widening towards pole and
416	equator, psilate to faintly microrugulate (SEM); colpus membrane nanoverrucate to granulate
417	(SEM).
418	Locality—Profen, Leipzig, Central Germany (Table 1).
419	Remarks—Form and sculpturing of pollen grains of this morphotype are remarkably similar
420	to those of Notanthera heterophylla (Feuer & Kuijt 1980, fig. 5). Notanthera heterophylla is one
421	of two species that comprise the two monotypic genera of the South American Notantherinae; a
122	subtribe of the Psittacantheae neither resolved as clade nor rejected with high support in
123	molecular-phylogenetic inferences (Grímsson, Grimm & Zetter 2017, files S1, S6). The
124	sculpturing of Profen MT2 is furthermore in line with the description and TEM image provided
125	by Feuer & Kuijt (1980).
426	Systematic note—The second species included in the Notantherinae, Desmaria mutabilis
127	(Poepp. & Endl.) Tiegh. ex B.D.Jacks, has not only a different pollen (Feuer & Kuijt 1980;
428	Grímsson, Grimm & Zetter 2017) but is also genetically distinct (Fig. 7).
129	Use as age constraint—This pollen can inform the minimum root age for the lineage leading
430	to Notanthera, i.e. the minimum age of the MRCA of Notanthera and Elytrantheae (scenarios 1-



431	3; preferred topology based on the taxon-reduced data set) or <i>Notanthera</i> and Psittacanthinae
432	(scenario 4; topology constrained to fit with Su et al. 2015, fig. 1B).
433	Profen MT3, pollen of the Elytrantheae clade (Figs 1K, 4C, 5C; Plate S09 in
434	File S3)
435	Description—Pollen, oblate, convex-triangular in polar view, no undistorted equatorial view
436	available, equatorial apices more or less truncated; pollen small, equatorial diameter 20.0-21.5
437	μm in LM, 19.2–20.0 μm in SEM; syn(3)colpate, colpi very narrow at equatorial apices,
438	widening towards the pole; exine 0.9–1.1 μm thick, nexine thinner than sexine (LM); tectate;
439	sculpturing psilate in LM, mostly nanobaculate to -echinate in area of mesocolpium in SEM,
440	bacula/echini 0.2-0.5 μm long, 0.1-0.2 mm wide (SEM); margo well developed, covering the
441	equatorial apices, mostly psilate, with few nanobacula/-echini in polar area, forming triangular
442	protrusions at pole (SEM); colpus membrane nanoechinate/-verrucate to granulate (SEM).
443	Locality—Profen, Leipzig, Central Germany (Table 1).
444	Remarks—The combination of characters (syncolpate with widening colpi, margo with
445	triangular protrusions and sculpturing reminiscent of the mesocolpium in polar area, sculpturing
446	of mesocolpium nanobaculate/-echinate) is today only found in members of the Elytrantheae.
447	With respect to studied modern Elytrantheae, the pollen of Profen MT3 resembles the most that
448	of Peraxilla tetrapetala (Fig. 4), but the sculpturing elements are more slender and higher (Fig.
449	5). The sculpturing in the mesocolpium (dimension and density of sculptural elements) matches
450	grains included in another morphotype found at Profen (Profen MT4; Fig. 5).
451	Use as age constraint—Here we used Profen MT3, MT4 and MT5 to constrain the root age of
452	the Elytrantheae, i.e. the minimum age of the MRCA of Notanthera and Elytrantheae (scenarios
453	1-3). Further studies of modern pollen of Elytrantheae at and below the genus level and more
454	genetic data are needed to decide whether the Profen MT3, and the related Profen MT4 and
455	MT5, are already indicative for a first divergence within the Elytrantheae and can be placed more
456	decisively within the Elytrantheae subtree.
457	



458	Profen MT4, possible pollen of the Elytrantheae clade (Figs 1L-O, 4D, 4E, 5D;
459	Plate S10, S11 in File S3)
460	Description—Pollen, oblate, concave-triangular to trilobate in polar view, no undistorted
461	equatorial view available, equatorial apices T-shaped; pollen small, polar axis 11.3–15.0 μm
462	long in LM, equatorial diameter 17.5–25.0 μm in LM, 14.3–20.0 μm in SEM;
463	demisyn(3)colpate, colpi short (SEM), widening towards the pole forming a polar depression
464	(polar sexine reduced); exine 1.1–1.3 μm thick, nexine thinner than sexine, nexine hexagonally
465	thickened in polar area (LM); tectate; sculpturing psilate in LM, mostly nanobaculate/-echinate
466	in SEM, bacula/echini 0.3–1.1 μm long, 0.1–0.4 μm wide at base (SEM); margo indistinct in
467	polar area, more prominent in equatorial regions, faintly microrugulate, covered by nanobacula/-
468	echini in polar area (SEM); colpus membrane nanoechinate/-verrucate to granulate (SEM).
469	Locality—Profen, Leipzig, Central Germany (Table 1).
470	Remarks— This pollen type has previously been figured (Manchester, Grímsson & Zetter
471	2015, fig. 2D-F), designated as Loranthaceae gen. et spec. indet. Sculpturing of Profen MT4 is
472	somewhat variable; dimensions, density and shape of sculptural elements resemble those in
473	Profen MT3 and Profen MT5 (see later), or are overlapping between both. Regarding its form
474	(trilobate with T-shaped equatorial apices) and lacking a distinct margo in the polar area, the
475	pollen differs from all modern members of the Elytrantheae. In this aspect, it is similar to the
476	pollen of Ligaria (Psittacantheae: Ligarinae), a genus with ambiguous phylogenetic affinities to
477	other New World genera (Grímsson, Grimm & Zetter 2017, file S1, figs S6-1-9). Also in
478	Ligaria, the sexine is reduced in the polar area (Fig. 4), the generally very narrow colpi are
479	fusing in a triangular polar depression (a feature only seen in Ligaria and its putative relative
480	Tristerix). Ligaria pollen grains are furthermore distinctly microbaculate (Fig. 5). Bacula are
481	found in all three Profen morphotypes linked to the Elytrantheae lineage, but are rare or absent in
482	the modern members of this clade.
483	Use as age constraint—See Profen MT3.
484	



485	Profen MT5, probable pollen of the Elytrantheae clade (Figs 1P, 1Q, 4F, 5E;
486	Plate S12 in File S3)
487	Description—Pollen, oblate, straight-triangular in polar view, elliptic to subrhombic in
488	equatorial view, equatorial apices broadly rounded; pollen small to medium, polar axis 7.5-11.5
489	μm long in LM, equatorial diameter 21.5-30.0 μm in LM, 18.7-24.4 μm in SEM;
490	demisyn(3)colpate, widening towards pole, terminating halfway between pole and equator
491	(SEM); exine 1.1-1.3 µm thick, nexine thinner than sexine (LM); tectate; sculpturing psilate in
492	LM, mostly nano- to microbaculate/-echinate in area of mesocolpium in SEM, bacula/echini 0.3-
493	$0.7~\mu m$ long, $0.1 – 0.3~mm$ wide at base; margo distinct but not raised, mostly psilate, with few
494	nanobacula/-echini in polar area, forming triangular protrusions at pole (SEM); colpus membrane
495	nanoechinate/-verrucate to granulate (SEM).
496	Locality—Profen, Leipzig, Central Germany (Table 1).
497	Remarks— The pollen fits with the morphotypes seen in modern members of the
498	Elytrantheae, although its combination of characters is unique. Small, demisyncolpate,
499	(sub)rhombic pollen grains are (so far) only known from Amylotheca, which differ from the
500	fossil pollen by their outline in polar view (Fig. 4) and sculpturing (Fig. 5). Regarding the latter,
501	Profen MT5 is very similar to grains included in Profen MT3. Both, Profen MT3 and MT5,
502	differ from the third morphotype with possible affinities to Elytrantheae (Profen MT4) by their
503	demisyncolpate grains (Fig. 4). Regarding the mesocolpium, Profen MT5 shows the densest
504	sculptured mesocolpium of all three morphotypes (Fig. 5).
505	Use as age constraint—See Profen MT3.
506	
507	Changchang MT, aff. Amyeminae vel Scurrulinae (Figs 1R, 1S, 6A, 6B, 6H, 6I;
508	Plate S13 in File S3)
509	Description—Pollen, oblate, concave-triangular to broadly trilobate in polar view, no
510	undistorted equatorial view available, equatorial apices broadly rounded; pollen small, equatorial
511	diameter 21.1–24.4 μm in LM, 19.1–21.8 μm in SEM; syn(3)colpate; exine 0.9–1.1 μm thick,
512	nexine thinner than sexine; tectate; sculpturing psilate in LM, nanoverrucate to granulate,
513	perforate in SEM, granula partly fused; margo well developed, psilate, widening towards the



14	equator, usually covering the entire apex (SEM); colpus membrane granulate; rhombic structures
15	(opercula) covering equatorial apices (SEM).
16	Locality—Changehang Basin, Jiazi Town, northern Hainan Island (Table 1).
17	Remarks—The minute sculpturing and its basic form link this pollen to the Lorantheae, in
18	particular to the Scurrulinae Taxillus and Scurrula (unresolved within Clade J) on one hand, and
19	Amyema (Amyeminae; Clade I in Vidal-Russell & Nickrent 2008a, sister clade of Clade J) on the
20	other hand. The pollen could be described as a Scurrulinae pollen with an Amyema-like margo. A
21	unique feature not found in any modern Loranthaceae so far are the operculum-like triangular
22	structures of the equatorial apices. Pollen of the two first diverging, long-branched lineages in
23	Lorantheae (Clades G and H in Vidal-Russell & Nickrent 2008a; cf. Su et al. 2015, figs 1B, S7;
24	Grímsson, Grimm & Zetter 2017, fig. 2) are markedly distinct. Thus, we think that this pollen
25	belongs to an extinct or ancestral Lorantheae lineage related to the core Lorantheae (= Clades I
26	and J according Vidal-Russell & Nickrent).
27	Use as age constraint—Based on its morphology, the Changchang MT could already
28	represent an early member of the Lorantheae core clade, i.e. would inform a minimum age of the
29	MRCA of Lorantheae core clade and its sisterclade Ileostylinae. However, some molecular data
30	sets indicate a sister relationship between Ileostylinae and Loranthinae (cf. Grímsson, Grimm &
31	Zetter 2017, files S1, S6). Furthermore, more information on pollen morphology in Lorantheae
32	would be needed to exclude the possibility that the Changchang MT is correctly recognised as a
33	representative of the Lorantheae core clade. Two of the four genera of the sister lineages of the
34	core Lorantheae (Loranthinae, Ileostylinae) have not yet been studied palynologically and little is
35	known on the other Amyeminae genera, the first diverging branch within the core Lorantheae.
36	Hence, we opted for a more conservative approach and used the Changchang MT to constrain the
37	MRCA of all Lorantheae.
38	
39	Theiss MT (Figs 1T-X, 2D; Plate S14, S15 in File S3)
40	Description—Pollen, oblate, trilobate in polar view, emarginate in equatorial view, lobes very
541 542	narrow, equatorial apices rounded; pollen small, polar axis 8.3-11.7 mm long in LM, 6.5-8.3 μm
342 343	long in SEM, equatorial diameter 10.0–15.0 μm in LM, 10.3–11.8 μm in SEM; demisyn(3)colpate; exine 0.9–1.2 μm thick, nexine thinner than sexine (LM); tectate; sculpturing
'+J	ucinisynto jeotpate, earne 0.7–1.2 mii tiilek, neame tiilinet tiidii seame (Livi), teetate, sculptuinig

PeerJ

544	psilate in LM, nano- to microverrucate in area of mesocolpium in SEM, verrucae often fused,
545	widely spaced, verrucae composed of conglomerate granula (SEM); margo well-developed,
546	covering nearly the entire surface of the grain in polar view, faintly microrugulate, granulate
547	(SEM); colpus membrane unknown.
548	Locality—Theiss, borehole southeast of Krems, Lower Austria (Table 1).
549	Remarks—This fossil pollen type has no direct modern counterpart. A unique feature is the
550	widely spaced verrucae in area of mesocolpium. Demisyncolpate grains evolved at least three
551	times in the Loranthaceae: in Amylotheca (Elytrantheae), in the Cladocolea-Struthanthus lineage
552	and Passovia (Psittacanthinae), and Tapinanthus (T. bangwenensis [Engl. & K.Krause] Danser,
553	T. ogowensis [Engl.] Danser; Lorantheae core clade). The fossil pollen shares no other features
554	with either Elytrantheae or Psittacanthinae. Grains with narrow (deflated) equatorial lobes, in
555	which the margo extends beyond the mesocolpial plane, are so far only known from several
556	members of the Lorantheae core clade (e.g. Englerina, Globimetula, Phragmanthera).
557	Mesocolpia with exclusively nanoverrucate to granulate sculpturing are only found in members
558	of the Lorantheae. For instance, the Tapinanthinae (core Lorantheae) Actinanthella has
559	emarginate, trilobate (to convex-triangular) pollen grains with a well-developed, mostly psilate
560	margo and nanoverrucate to granulate mesocolpium, but they differ from the fossil pollen by
561	their size and zonocolpate apertures.
562	Use as age constraint— Due to the unique morphology, yet superficial knowledge about
563	pollen evolution in Lorantheae (see Changchang MT), we decided against using the Theiss MT
564	to constrain a node higher up in the tree (e.g. the MRCA of Tapinanthinae and Emelianthinae).
565	
566	Altmittweida MT, aff. Helixanthera (Figs 1Y-Ä, 6C, 6D, 6J; Plate S16 in File
567	<i>S3)</i>
568	Description—Pollen, oblate, convex-triangular in polar view, emarginate in polar view,
569	equatorial apices broadly obcordate; pollen small, polar axis 4.4-5.5 µm long in LM, equatorial
570	diameter 14.4–17.8 μm in LM, 13.7–16.0 μm in SEM; syn(3)colpate; exine 0.9–1.1 μm thick,
571	nexine thinner than sexine, intercolpial nexine thickening at pole, sexine partly reduced in polar
572	area (SEM); tectate; sculpturing psilate in LM, nano- to microverrucate, granulate in SEM,



73	verrucae composed of conglomerate granula (Fig. 6J); margo psilate to microverrucate,
74	granulate; colpus membrane nanoverrucate to granulate (SEM).
75	Locality—Altmittweida, Saxony, Germany (Table 1).
76	Remarks—This pollen type has previously been figured by Kmenta (2011, plate 11, figs 1–3)
77	as "Loranthaceae gen. et spec. indet." Pollen very similar to this fossil pollen can be found in two
78	extant species of the Lorantheae: Amyema gibberula (type genus of Amyeminae, Clade I
79	according Vidal-Russell & Nickrent 2008a) and Helixanthera kirkii (Grímsson, Grimm & Zetter
80	2017). Both species are similar in outline (convex-triangular, emarginate) and sculpturing
81	(margo indistinct, with similar sculpturing than adjacent mesocolpium). In LM, Amyema shows a
82	distinct hexagonal thickening of the polar nexine, whereas in Helixanthera the thickening covers
83	a larger area of the grain and is most dominant in the intercolpial areas; the latter can be seen in
84	the fossil pollen. The flanks of the equatorial apices in the equatorial plain are straight in
85	Helixanthera and the fossil, whereas they are continuously curved in Amyema. In addition, the
86	polar depression in Helixanthera and the fossil are identical in all details in SEM (Fig. 6C, D, F),
87	whereas in Amyema the polar margo is more distinct and shows three small triangular protrusions
888	(Fig. 6E).
89	Use as age constraint—The phylogenetic position of Helixanthera within the core Lorantheae
90	is uncertain. Nucleotide data has been produced for three species including H. kirkii, but the data
91	are partly problematic and too fragmentary. Helixanthera kirkii (only nuclear data available, only
92	species palynologically studied so far) nests deep within the Lorantheae core clade, and H .
93	parasitica (only plastid data available) is sequentially divergent from all Lorantheae and
94	effectively unplaced (see Fig. 7 and File S1 for further details). The third and best covered
95	species, H. coccinea, groups with species of Dendrophthoe in agreement with the current
96	systematic scheme, but its pollen is yet to be studied. Thus, <i>Helixanthera</i> has not been included
97	in the taxon-reduced species-consensus dataset used here for the molecular dating. A
98	conservative use could be constraining the minimum age of the MRCA of the Clade J (i.e.
99	Scurrulinae, Dendrophthoinae, Emelianthinae, and Tapinanthinae; see Discussion).



601

Inferences

						/ - -	_\
Racic cianal	ın	tha	horusetad	malacular	doto	/Lia	/ 1
Dasil Siuliai		LIIC	IIAI VESLEU	IIIVIELUIAI	uala	I FIU.	,
Basic signal						(-	•

602	Our inferences, based on species-consensus sequences and different sets of data (see File S1
603	and files included in OSA), did not reveal any well-supported conflict between the nuclear and
604	plastid gene regions. Inclusion or exclusion of the most divergent, length-polymorphic non-
605	coding (plastid) trnLLF region showed little effect on the optimised ML topologies and BS
606	support values. When not including any long-branching outgroups, the data largely fails to group
607	the root parasitic taxa. Hence, there is a lack of support for a root parasitic grade. An according
608	subtree (e.g. Su et al. 2015, fig. 1B) draws its support exclusively from the matK gene data and is
609	enforced if long-branching sistergroups of the Loranthaceae are included (Grímsson, Grimm &
610	Zetter 2017, file S6). Overall, the single- and oligo-gene species-consensus trees showed the
611	same principal topology as earlier found using genus-consensus sequences (Grímsson, Grimm &
612	Zetter 2017, figs 2, 3). However, species of the same genus were not necessarily reconstructed as
613	siblings. In the case of Helixanthera, Psittacanthus (nuclear and plastid data), and Plicosepalus
614	(plastid data only), the branches separating the putative siblings received no high support, while
615	the opposite was true for Amyema, Tapinanthus (nuclear and plastid data), Amylotheca,
616	Lepidaria, and Oncocalyx (plastid data only). In terms of genetic-phylogenetic distances, the
617	species of Helixanthera show the least coherence at the genus level. Aside from this, several
618	clades were consistently reconstructed and usually received moderately high to unambiguous
619	support (BS \geq 70) from different data sets (Fig. 7): (i - iv) the Old World Lorantheae with three
620	subclades (Loranthinae, Ileostylinae, core Lorantheae), (v-vi) the Amyeminae (except
621	Baratranthus axanthus) and Scurrulinae within the core Lorantheae; (vii) the New World
622	Psittacanthinae (except for Aetanthus, which is poorly sampled in our data set); and (ix) the
623	Elytrantheae (poorly supported based on nuclear data due to faint discriminating signals). The
624	positions of the other mostly monotypic genera of the family remained unresolved; alternative
625	splits representing deep relationships generally received low support. Bayesian inference is more
626	decisive, with PP ~ 1.00 found for all major splits with moderately high to high BS support
627	$(BS_{ML} \ge 77)$ and several splits with low BS support (see <i>Material & Methods</i>). Some of the
628	deepest splits that received BS $_{ML}$ < 35, received PP > 0.5 (all alternatives with PP < 0.2). A split
629	between root and aerial parasites is not supported by any analysis with $BS_{ML}/PP > 20/0.2$. A



detailed account regarding topological ambiguity of inferences using the currently available molecular data can be found in File S5.

The divergence in the covered gene regions is substantial (see branch-lengths in Fig. 7); the resulting terminal 'noise' appears to obscure any signal that may allow for the discrimination of deeper phylogenetic splits. This may explain to some degree, in addition to the relatively high proportion of missing data, the low resolution capacity of comprehensive species-level data sets. When the taxon set was reduced to only those species with full data coverage, support along the backbone and towards the leaves of the Loranthaceae tree increased. This reduction also showed a positive effect on the dating: using the complete taxon set and matrices with numerous data gaps, ESS values converged very slowly (rooting scenarios 1 and 3) or not at all (rooting scenario 2; see also File S1).

Alternative clock-based roots

For four of the five comprehensive datasets (all taxa, different sets of gene samples), the clock-inferred root was placed between the predominately Old World Lorantheae and a mostly southern hemispheric, American-Australasian clade collecting all three root parasitic genera and the members of the other two aerial parasitic tribes, the (probably paraphyletic) Psittacantheae and (putatively monophyletic) Elytrantheae (Table 2). In the case of the most-inclusive data set (all taxa, all gene regions), the root was shifted by two nodes and placed within the Lorantheae subtree, splitting the genetically divergent subtribes Loranthinae and Ileostylinae from the remainder of the Lorantheae (= Clade J according to Vidal-Russell & Nickrent 2008a). The subsequent evolutionary scenario would imply that root parasites and other southern hemispheric lineages share an ancestor with only the Loranthinae and Ileostylinae. This would mean a paraphyletic Lorantheae tribe, which is highly unlikely (Nickrent et al. 2010; Su et al. 2015; Grímsson, Grimm & Zetter 2017). Thus, this alternative root was not further considered. In contrast to these roots, the taxon-reduced, less "gappy" dataset (42 species covering, at least partly, all included gene regions) recovered the outgroup-inferred root, with *Nuytsia* as sister to all other loranths.



Following our clock-rooting results and those of earlier studies, we applied three different 658 659 root constraints to judge potential effects of topological uncertainties regarding the primary 660 relationships on the dating estimates. In addition, we constrained our data to the topology of the Loranthaceae subtree as shown in Su et al. (2015; scenario 4), which – according to an expert on 661 the group – is the most correct one to date (but see Grímsson, Grimm & Zetter 2017, file S6). We 662 find that independent of the position of the root and exact structure of the backbone topology, 663 664 primary divergences in Loranthaceae were terminated by the end of the Eocene at the latest (Table 3). The posterior estimates of the evolutionary rates per gene were equivalent in all 665 666 rooting scenarios (Table 4) and slightly higher for the fourth scenario in which the topology was constrained to the one of Su et al. (2015). The estimated rates for matK and trnLLF were within 667 668 the range of mean rates reported for coding and non-coding plastid gene regions (7*10⁻⁵–8*10⁻³ substitutions per million years; e.g. Wolfe, Li & Sharp 1987; Palmer 1991; Guzmán & Vargas 669 670 2010; Désamoré et al. 2011; Chen et al. 2012; Lockwood et al. 2013) The robustness of our 671 estimations are further supported by the fact that the observed phases of increased diversification 672 (number of coexisting lineages) and stagnation concur with key events in Cenozoic climate and 673 vegetation evolution (Fig. 8). Most crown group radiation, the formation of the modern genera, apparently happened no later than the Miocene. Based on the limited species coverage, it is 674 impossible to estimate when intra-generic radiation stepped in, and at which point closer related 675 676 genera became isolated and diverged. 677 Comparison of Bayes factors showed that rooting scenario 3, the pollen-informed root, is 678 decisively superior (according Kass & Raftery 1995) than the tested alternatives (Table 5). Thus, 679 we chose rooting scenario 3 as the basis for our discussion and conclusion. The divergence 680 between *Tupeia* (A-type pollen) and Loranthaceae with B-type pollen is placed in the early 681 Eocene (~50 Ma; Fig. 9, Table 3). A primary radiation followed shortly after (less than 2 myrs), 682 and involved the formation of an essentially Old World (Lorantheae) and New World clade (root parasites, Elytrantheae, Psittacantheae). Subsequently, the first divergences in the New World 683 clade occurred (> 43 Ma; Fig. 9). Crown group radiation in the Lorantheae started in the late 684 685 Eocene (≥ 38 Ma) at the latest; the subclades and monotypic lineages (subtribes Psittacanthinae, Ligarinae, Notantherinae) of the probably paraphyletic Psittacantheae diverged at about the same 686 687 time. A second major radiation phase took place ~10 myrs later (latest in the Oligocene) and

Temporal framework for pollen evolution in Loranthaceae (Figs 8-9; Table 3)



695

- involved the Old World core Lorantheae (subtribes Amyeminae, Dendrophthoinae,
 Emelianthinae, Scurrulinae, Tapinanthinae) and New World Elytrantheae. Crown group
 radiation, the formation of lineages equalling most modern genera, commenced at about the
 same time and lasted till the mid-Miocene (≥ 9 Ma). In general, the genera root deeper, i.e. are
 older, in the (mostly) South American Psittacanthinae than in the Old World Lorantheae
 sublineages and the (mainly) Australasian Elytrantheae. Generic diversification culminates in the
 - Historical Biogeography (Figs 10-11)

early to mid-Miocene, a time of ameliorated global climate.

696 Pollen studied using SEM and subsequent node dating (Figs 8, 9; Table 3) indicate that 697 several major lineages of Loranthaceae were present in the Northern Hemisphere by the middle 698 Eocene (Fig. 10A). The Eocene pollen record includes representatives of extinct or ancestral 699 lineages with affinities to root-parasitic genera such as *Nuvtsia*/Nuvtsieae, but possibly also to 700 the Lorantheae (Miller Clay Pit MT1, Stolzenbach MT, Profen MT1). In addition, today's 701 exclusively epiphytic lineages are present: Psittacanthinae in North America/Greenland (Miller 702 Clay Pit MT2, MT3, Aamaruutissaa MT), *Notanthera* and Elytrantheae in Central Europe 703 (Profen MT3, MT4 and MT5), and core group Lorantheae in East Asia (Changchang MT). All 704 these records represent the earliest unequivocal fossil records of their respective groups. At least 705 one of these lineages, the ancestral/extinct lineage bridging the root parasites and Lorantheae, 706 persisted in Eurasia during the late Eocene and Oligocene (Theiss MT, Altmittweida MT; Fig. 707 10B) until today. These younger pollen types, which were not used as node age priors, are in 708 good agreement with the dating estimates (Fig. 9). Furthermore, we noticed that none of the 709 putatively derived pollen morphologies characteristic of certain members of the Psittacanthinae (compact B-type, C-type and D-type pollen) and Lorantheae (Loranthinae, Tapinanthinae-710 711 Emelianthinae; ± compact B-type pollen, B-type pollen with minute sculpturing, heteropolar 712 grains) have been found (so far) in the older strata. Pollen records from the Miocene onwards, 713 studied using LM and possibly representing a large range of Loranthaceae lineages with a B-type pollen, fall within the modern distribution area (Fig. 11), and potentially include such B types 714 (File S4). The most derived C- and D-type pollen characteristic for *Dendropemon*, *Passovia* p.p. 715 716 and Oryctanthus, which should be straightforwardly recognised with LM only, is rare and only 717 known from late Miocene/sub-recent sedimentary rock formations. The dated trees predict an



718	Oligocene/early Miocene age for the MRCA of Passovia pyrifolia and Oryctanthus (Fig. 9). If
719	Loranthaceae with A-type pollen contributed to the pollen record of the family, they would not
720	have been recognised as Loranthaceae, hence, are not included in our maps and File S4.
721	Well-resolved major clades of Loranthaceae are restricted to one or two adjacent
722	biogeographic regions (Fig. 11). Except for Nuytsia/Nuytsieae (today only found in southwestern
723	Australia), the fossil pollen records essentially reflect the modern situation, only extending the
724	range of the respective New World and Old World lineages to higher latitudes of the Northern
725	Hemisphere.
726	
727	Discussion
728	Diagnostic value of Loranthaceae pollen for tracing modern lineages back in
720	time

729 Pollen of various modern Loranthaceae have been studied using light (LM), transmission 730 731 electron- (TEM) and scanning-electron microscopy (SEM) (Feuer & Kuijt 1978; Feuer & Kuijt 732 1979; Feuer & Kuijt 1980; Feuer & Kuijt 1985; Kuijt 1988; Liu & Qiu 1993; Han, Zhang & Hao 733 2004; Roldán & Kuijt 2005; Caires 2012; Grímsson, Grimm & Zetter 2017). In general, pollen of 734 Loranthaceae – and other Santalales – reflect phylogenetic relationships and geneticphylogenetic distances (Grímsson, Grimm & Zetter 2017), which make them a valuable asset for 735 736 biogeographic and dating studies. Some genera of putatively early diverging Loranthaceae 737 lineages such as *Nuytsia* (monotypic Nuytsieae), *Atkinsonia* (bitypic Gaiadendreae, not resolved 738 as clade in the molecular trees), the Psittacantheae Notanthera (bitypic Nothanderinae), Ligaria 739 and Tristerix (Ligarinae, not resolved as sibling genera), and Tripodanthus, Dendropemon, Orycanthus and Passovia p.p. (Psittacanthinae), show unique pollen types that have not been 740 741 found in any other studied genus so far. Moreover, there is no indication that identical/highly 742 similar pollen types evolved convergently in non-related Loranthaceae (or other Santalales). 743 Non-unique pollen types are typically found in genera which are either part of the same, well-744 supported molecular clade (core Lorantheae; Elythrantheae; Psittacanthinae subclades), or shared 745 with genera where the molecular data is indecisive regarding their exact phylogenetic position

(Grímsson, Grimm & Zetter 2017; this study).

746



47	Even though the modern situation makes it unlikely that – in the past – extinct lineages of
48	Santalales or Loranthaceae have produced pollen mimicking those of modern, extant, but not
49	closely related lineages, one needs to consider the possibility that a modern genus may have kept
50	a more primitive ('plesiomorphic') pollen type of its evolutionary lineage. The Eocene and
' 51	Oligocene pollen grains documented in this study show morphologies (i) not found in any
52	modern taxon studied so far (Stolzenbach MT, Profen MT1, Theiss MT), or (ii) found
53	exclusively in a single modern genus (monotypic Nuytsia: Miller Clay Pit MT1, Tripodanthus
54	with three extant species: Miller Clay Pit MT2, MT3, Aamaruutissaa MT; monotypic
'55	Notanthera: Profen MT2; phylogenetically problematic, see Fig. 7; Helixanthera: Altmittweida
56	MT), or (iii) are limited to a modern lineage (Elytrantheae: Profen MT3-5; core Lorantheae:
57	Changehang MT) with none of the other modern species studied so far having an identical
'58	pollen. On the other hand, we found no pollen in our Eocene and Oligocene assemblages
'59	representing current-day diverse and widespread genera (such as Loranthus in Eurasia).
60	Extinct or ancestral pollen morphs of the Eocene and Oligocene of Europe—The shared
61	pollen type of the South American root parasite Gaiadendron and the eastern Australian
62	Lorantheae Muellerina (one of two genera in the subtribe Ileostylinae; the other has not been
63	palynologically studied thus far) is a candidate for an ancestral, primitive and shared
64	('symplesiomorphic') morphology. The pollen of these two genetically and morphologically
65	distinct modern genera are indistinct (Nickrent et al. 2010; Su et al. 2015, fig. 2; Grímsson,
'66	Grimm & Zetter 2017). The distinctly striate margo is a feature only seen in a few isolated, early
67	diverging (Eocene) modern species/genera of ambiguous phylogenetic affinity (Fig. 9, Table 3).
68	So far, no modern species showed an intermediate pollen type between the putatively
69	plesiomorphic Gaiadendron-Muellerina pollen and the derived pollen characterising other
70	members of the Lorantheae, e.g. the characteristically weakly oblate pollen of <i>Loranthus</i> . The
71	Stolzenbach MT, Profen MT1, and Theiss MT of the Eocene and Oligocene of central Europe
72	are equally small and share certain ornamental characteristics with the pollen of Gaiadendron-
73	Muellerina such as a distinctly striate margo. Deviating features, e.g. more minute sculpturing of
74	the mesocolpium, are shared with other members of the Lorantheae. This could make them
75	candidates for an extinct lineage related to Lorantheae or ancestors of the Lorantheae subclades.
76	At about the same time, more derived Lorantheae pollen grains can be found in the Eocene of
77	East Asia (Changchang MT) and the Oligocene of Germany (Altmittweida MT), with clear



//8	arimities to the core Lorantheae. This provides conservative minimum estimates for the
779	Lorantheae crown age, i.e. the divergence between Loranthinae, Ileostylinae, and core
780	Lorantheae. Our dating estimates also indicate that there was a time gap of ca. 10 myrs between
781	the formation and initial radiation of the Lorantheae and their subsequent diversification (Fig. 9,
782	Table 3). Our current working hypothesis is that the Stolzenbach MT, Profen MT1, and Theiss
783	MT, do in fact represent extinct sister lineages or precursors of the modern Old World
784	Lorantheae (e.g. the Loranthinae). Whether these Loranthaceae extended into Africa or not, is
785	unknown. The divergence between the East Asian Scurrulinae and the mostly African
786	Tapinanthinae and Emelianthinae is placed in the Oligocene (Fig. 9), a time when substantial
787	global cooling triggered the retreat of subtropical and tropical forests to low latitudes (Mai 1995;
788	Zachos et al. 2001). This event may have triggered the isolation between both clades and lead to
789	the extinction of the ancestral pollen morphologies. Unfortunately, Africa is palaeo-
790	palynologically understudied, so we do not know at which time the African Lorantheae with
791	pollen grains typical for their modern members established. SEM studies of African palynofloras
792	with Loranthaceae pollen from the Oligocene to Pliocene are desperately needed.
793	Pollen of Tripodanthus, a putative living palyno-fossil—Another case of a modern genus
794	that conserved a primitive pollen morphology is evident from the Eocene pollen from North
795	America and Greenland (Miller Clay Pit MT1, MT2; Aamaruutissaa MT). These pollen are
796	highly similar to identical to pollen of two out of three species of the modern South American
797	genus Tripodanthus; the third species has a more compact pollen somewhat similar to that of
798	small-flowered species of the Psittacanthinae (Fig. S4; Feuer & Kuijt 1985; Roldán & Kuijt
799	2005; Amico et al. 2012; Grímsson, Grimm & Zetter 2017). <i>Tripodanthus</i> is one of the earliest
300	diverging Psittacanthinae (Figs 7, 9; Vidal-Russell & Nickrent 2008a; Grímsson, Grimm &
301	Zetter 2017). Pollen in the other represented genera of the Psittacanthinae (Passovia,
302	Dendropemon, Struthanthus, Oryctanthus) appear strongly derived in comparison to that of
303	Tripodanthus and part of Psittacanthus (Feuer & Kuijt 1979; Feuer & Kuijt 1985), and include
304	types that could be identified under LM. However, such pollen have not yet been reported from
305	the fossil record except for the youngest strata (Bartlett & Barghoorn 1973; Graham 1990; File
306	S4). Moreover, the current molecular data covers only a very limited fraction of the species in
307	the Psittacanthinae, a clade palynologically well studied and diverse. So, at the moment, we lack
808	a sound molecular framework to test hypotheses about pollen evolution within the group, and the



820

821

822

823

824

825

826

827

828

829

830

831

832

833

834

835

836

837

838

809 group is genetically undersampled. Even so, our set of ML inferences highlights the shortcoming 810 of the current generic concepts used for the group (Fig. 7; Files S1, S5). 811 In conclusion, the Eocene Tripodanthus-like pollen of North America and Greenland might 812 have been produced by extinct or ancestral members of the Psittacanthinae, rather than an 813 ancient member of the *Tripodanthus*-lineage. It may merely confirm the existence of the New World Psittacanthinae clade in the Eocene of North America and Greenland, and should be 814 815 linked with a deeper node. Using LM, Loranthaceae pollen (Gothanipollis sp.) has been recorded 816 from North and South America from the early Eocene onwards (File S4 lists 17 records), which may well reveal different forms of Psittacanthinae pollen, or of less diverse New World lineages 817 818 when re-studied using SEM.

Data-inherent shortcomings

The data assembled for our study from gene banks do not allow for conclusions at and below the genus level to be drawn. Genus-level data are limited, and in several cases where more than a single species (or individual) has been sequenced from the same genus, the genera do not show a high coherence when it comes to tree inferences (Fig. 7). This will become a problem when studying pollen grains from younger strata, which, increasingly, may show forms identical to one or more modern genera. For instance, our assessment of the Altmittweida MT is based on its similarity to the pollen of Amyema and Helixanthera figured in Grímsson, Grimm & Zetter (2017). In that study, material was used from youchers identified as Amyema gibberula, the only species of the Amyeminae clade studied so far palynologically, and *Helixanthera kirkii*. According to our species-level analyses, species of neither of the two genera are resolved as sibling species. As exemplified in Figure 7, the two or three sequenced species of Amyema are resolved at different placements in the Amyeminae subtree, but A. gibberula has not been sequenced at all. Helixanthera kirkii has only been sampled for nuclear data, and is placed far (phylogenetically speaking) from its congeners, which are scattered across the core Lorantheae subtree. Lacking any comparative data it cannot be judged if these placements are genuine, or if one (or several) of the species (sequenced individuals) were misidentified/-associated (generic concepts are volatile in Loranthaceae, see synonymy lists provided by Tropicos, org 2016). Thus, based on the available pollen of the Lorantheae and their established genetic affinities as members of the same clade, we can only assume with some certainty that the Altmittweida MT is



839	a likely representative of the core Lorantheae, but not if it is a congener of <i>Helixanthera</i> , or more
840	closely related to part of that genus. We also cannot judge to which degree Helixanthera pollen
841	can be considered derived/unique enough within the core Lorantheae to warrant the association
842	of a fossil pollen with a single extant genus.
843	Furthermore, we can only rely on fossil pollen of several northern hemispheric localities;
844	localities we have been studying in the recent years. But most of the extant, and potentially
845	extinct, diversity of Loranthaceae lies in the Southern Hemisphere (Figs 10-11). South America,
846	and in particular Africa, are much less studied palynologically than e.g. Europe, and the tradition
847	of using SEM to study fossil pollen records is scant or absent in the Americas and Australasia
848	(but see Ferguson et al. 2009; Bouchal, Zetter & Denk 2016; del Carmen Zamaloa & Fernández
849	2016). Nevertheless, there are records of Loranthaceae pollen from these areas, and if Antarctica
850	is included (File S4), these records cover anything between the early Eocene and Holocene.
851	Moreover, pollen assigned to Santalaceae or Viscaceae under LM may in fact be Loranthaceae
852	Pollen Type A. Re-studying at least some of these assemblages using high-resolution SEM
853	photography could provide much needed evidence for the distribution of different Loranthaceae
854	lineages back in time. A more detailed and comprehensively studied pollen record at a global
855	scale would also provide the necessary number of fossils to put forward and test explicit
856	phylogeographic scenarios for the family. In the case of South America, particular fossil pollen
857	can be straightforwardly compared to the substantial variation seen in the modern genera and
858	species (seminal works of Feuer & Kuijt, 1979, 1980, 1985). It would be most interesting to
859	pinpoint the earliest occurrences of the compact B-type pollen characteristic of the Cladocolea-
860	Struthanthus lineage or the strongly derived C- and D-type pollen of the Passovia pyrifolia-
861	Dendropemon-Orycthanthus clade. However, we are missing comprehensive molecular data on
862	the Psittacanthinae at the intra-generic level and on species included in <i>Passovia</i> and <i>Phthirusa</i>
863	(according Kuijt 2011; see e.g. Fig. 7). A detailed molecular-phylogenetic framework would be
864	necessary to depict evolutionary trends in pollen morphology of this group and to identify
865	ancestral, more primitive (plesiomorphic) vs. modern, derived (apomorphic) pollen morphs of
866	this lineage in the fossil record. Correlation of such data with palaeovegetational evidence
867	(accompanying flora, in particular availability of mid- to high-canopy trees), may help to assess
868	if the shift from root to aerial parasitism in currently exclusively aerial parasitic Loranthaceae
869	lineages occurred before or after their establishment.

871

872

873

874

875

876

877

878

879

880

881

882

883

884

885

886

887

888

889

890

891

892

893

894

895

896

897

898

899

Due to the data-related limitations regarding both the molecular data and the fossil record, our dating analysis set-up can only provide absolute minimum estimates for divergence ages in the Loranthaceae. In a recent study on Osmundaceae, we observed that uncorrelated clock-inferred dates deviated from dates inferred with the recently proposed fossilised-birth-death dating approach (FBD; Heath, Huelsenbeck & Stadler 2014), with the former tending to underestimate age (Grimm et al. 2015). In contrast to traditional node dating, FBD dating recruits the entire fossil record of a focal group and seems to outperform node dating in simulation and with realworld data (Heath, Huelsenbeck & Stadler 2014; Grimm et al. 2015; Renner et al. 2016). In the case of Loranthaceae, the coverage of lineages with fossils and of the modern taxonomic diversity is insufficient for the application of FBD, although this approach would allow for a more appropriate handling of the fossils (including ours), namely as members of lineages, rather than minimum age priors for discrete MRCA. To avoid over-interpretation of the fossils during the latter, all fossil age constraints and estimates were used here in a conservative manner (see Descriptions; Inferences). More precise estimates and a larger taxon set would be needed to reconstruct explicit migration pathways of the different Loranthaceae lineages that consider the fossil record of the family.

Timing of evolution of main Loranthaceae lineages

The main, currently aerial parasitic lineages, of Loranthaceae evolved about 20 myrs earlier (Table 3) than estimated by Vidal-Russell & Nickrent (2008b); a discrepancy easily explained. In contrast to the earlier study, we can exclusively rely on ingroup fossils as age constraints, which provide direct evidence for the occurrence of several Loranthaceae lineages in the middle Eocene. Vidal-Russell & Nickrent (2008b) used two sets of fossil constraints for their dating of an all-Santalales dataset. The first set used a single fossil (*Anacolosidites* Cookson & K.Pike) to constrain the root age of an Olacaceae s.l. subclade, the former Anacolosideae (=Aptandraceae), to 70 Ma, providing generally older estimates than the second, preferred set. The second set used five additional fossils and included *Cranwellia* S at.K.Srivast to constrain the root age of Loranthaceae to >70 Ma. We again diverged from Vidal-Russell & Nickrent (2008b), by not using a different study, i.e. Wikström, Savolainen & Chase (2001), to constrain the (ingroup) root age. Using secondary dating constraints and age priors based on outgroup fossils typically leads to overly young age estimates (e.g. Grimm & Renner 2013, for Betulaceae; Garzón-Orduña





900	et al. 2015, for Solanaceae and Ithomini). For example, in the two families of Canellales,
901	namely Canellaceae and Winteraceae, crown group estimates using ingroup fossils as age priors
902	are about double the age of those inferred based on a large magnoliid dataset including only root
903	age constraints for the Winteraceae and the order (Marquínez et al. 2009; Thomas et al. 2014;
904	Massoni, Couvreur & Sauquet 2015; Müller et al. 2015).
905	It must be noted that the existence of a lineage, as evidenced by the pollen record, does not
906	allow for conclusions to be drawn regarding the parasitic habit of its extinct members. The
907	Muellerina-Gaiadendron case shows that similar pollen grains are produced by root and aerial
908	parasites. Even if we consider this pollen type to be primitive ('symplesiomorphic'), the shift of
909	the Lorantheae to aerial parasitism did not affect the pollen morphology in all of its sublineages
910	to the same degree. The unconstrained topologies indicate several shifts from root to aerial
911	parasitism within the family. It may thus be possible that more shifts occurred in the past than
912	visible from the present-day situation. Ancient members of a Loranthaceae lineage may have
913	been root parasites (or intermediate) in contrast to their modern representatives. Our older
914	estimates nevertheless make sense considering the substantial genetic divergence between extant
915	Loranthaceae, the backdrop of Cenozoic global climate evolution, and the evolutionary history of
916	the potential hosts for aerial Loranthaceae: mid- to high-canopy trees (see also Fig. 8). Although
917	some species of the Loranthaceae family seem to be linked to a specific host, the genera
918	themselves usually parasitise a wide range of hosts, spanning different families and even orders
919	(File S6). The colonisation potential of aerial mistletoes is high. For instance, the New Zealand
920	endemic Ileostylus micranthus (Lorantheae: Ileostylinae) parasitises 47 different families,
921	including northern hemispheric lineages introduced in historic times (Norton & de Lange 1999).
922	Australian mistletoes commonly infest two widespread, common and native tree genera (Acacia,
923	Eucalyptus), but in total 256 genera are infested, and species of four genera can be found on
924	exotic (introduced) tree genera such as Nerium, Quercus (oaks), Platanus, and Salix, among
925	others (Downey 1998). All these genera are potential hosts of northern hemispheric
926	Loranthaceae (e.g. Loranthus europaeus), and can be traced back at least to the Eocene (e.g. Mai
927	1995). For example, primary radiation and diversification of oaks – the most diverse,
928	extratropical tree genus of the Northern Hemisphere with more than 400 modern species (Nixon
929	1997; Huang, Zhang & Bartholomew 1999) – was finished by the end of the Eocene (Hubert et
930	al. 2014). The general vegetation types in which aerial Loranthaceae are found – various sorts of





931	subtropical to temperate, non-trost forests but also tropical blomes – have been available through
932	the entire Cenozoic (e.g. Mai 1995). Most of the Eocene is characterised by a globally
933	ameliorated climate (Zachos et al. 2001). During this time scale, tropical and subtropical forests
934	reached a peak in their distribution, with subtropical and temperate forests reaching far north.
935	This could have been the trigger for a global radiation of aerial parasites in Loranthaceae. In
936	western Greenland, currently epiphytic Loranthaceae (Psittacanthinae; Aamaruutissaa MT, aff.
937	Tripodanthus) co-occurred with a high variety of subtropical to temperate Fagaceae including
938	various intrageneric groups of oaks (Grímsson et al. 2015). Fagaceae in general (see File S6) and
939	oaks in particular are natural hosts of Eurasian Lorantheae. Oaks are major elements of
940	extratropical northern hemispheric mid- to high-canopy forests and open woodlands The
941	Aamaruutissaa palynological assemblage covers representatives of ca. 30 families of woody
942	angiosperms in total (Grímsson et al. 2014b), including many potential hosts of epiphytic
943	Loranthaceae in modern-day extra-tropical North America and East Asia. The arborescent
944	families Fagaceae, Juglandaceae, and Sapindaceae (including maples, Acer) can be found at all
945	other localities included in our study (Table 1, File S7). All LM/SEM palynologically studied
946	floras further comprise lianas (Vitaceae) and additional predominately or exclusively arborescent
947	families such as Aquifoliaceae (Ilex), Cornaceae, Malvaceae, Myricaceae, Oleaceae,
948	Platanaceae, and Ulmaceae. On the other hand, typically or exclusively herbaceous families are
949	rare (or absent). Thus, the early Loranthaceae described here apparently thrived in densely
950	forested habitats with ample niche opportunities for aerial parasites.
951	The mid-Oligocene falls into a phase of global cooling and retreat of subtropical and tropical
952	vegetation belts to lower latitudes. If the main currently aerial parasitic lineages evolved during
953	that time in Australia, as inferred by Vidal-Russell & Nickrent (2008a, 2008b; but see Barlow
954	1990 and Vidal-Russell & Nickrent 2007), Loranthaceae would have needed to be extremely
955	competitive to radiate at a global scale. With its (cold-)temperate to polar climate from the
956	Oligocene onwards, Antarctica is an unlikely corridor for the global radiation of Loranthaceae.
957	The situation in eastern North America and Europe, two areas heavily affected by the Pleistocene
958	climate fluctuations, indicates that Loranthaceae cannot compete with their distant sister clade
959	Viscaceae in the temperate zone, and there is no indication that any Loranthaceae lineage ever
960	thrived in cold-temperate/boreal climates. Long-distance dispersal via Africa or the Pacific is
961	unlikely in the light of the modern distribution patterns (Fig. 11). All continental African species



962	are members of the core Lorantheae, and distant relatives of the exclusively Australasian and
963	South American lineages. The age estimates indicate that main Australasian (probably
964	monophyletic Elytrantheae) and New World lineages (probably paraphyletic Psittacantheae)
965	diverged around the same time (Fig. 8; Table 3), which would fit with the traditional Gondwana
966	Breakup scenario suggested for the family (Barlow 1990; Vidal-Russell & Nickrent 2007).
967	Whether divergences in Loranthaceae are triggered by actual tectonic events has to be tested
968	once a more comprehensive taxon and gene sample is available, and would require a re-
969	investigation of the pollen record of the Southern Hemisphere using combined LM and SEM
970	microscopy. With such data at hand, explicit pollen evolution scenarios could be established to
971	discriminate between pollen indicative of ancestral or deep-rooting, slow-evolving (regarding
972	their pollen morphologies) modern lineages, and extant genera or relatively late radiated
973	supergeneric groups. The Oligocene cooling may have been the final trigger to isolate the
974	American lineages from those in the Old World and Australasia. It also may have effected
975	transcontinental exchange between Africa and East Asia, trigger the formation of the
976	contemporary genera (Fig. 9, Table 3, but see Discussion section before), and manifest the
977	isolation of Australasian lineages.

Conclusion

Molecular age estimates have often been criticised as being too young in comparison to the
fossil record. The crown group radiation and associated onset of aerial parasitism in
Loranthaceae, placed in the middle Oligocene by a study including all lineages of the Santalales
(Vidal-Russell & Nickrent 2008b), could have been taken for such a case. It would have invoked
three difficult-to-understand phenomena: (i) Quick long-distance dispersal and rapid radiation on
a global scale of a mostly tropical-subtropical lineage during a phase of global cooling. (ii) Host-
specialisation and simultaneous colonisation of subtropical forest elements that were already
evolved by the Eocene, at least 20 myrs earlier. (iii) The comparatively rich palynological record
of the zoophilous Loranthaceae, with earliest reliable records in the Eocene of Australasia
(south-eastern Australia, Tasmania), East Asia (Hainan, southern China), western Eurasia
(Germany), the Americas (Argentina, southeastern United States) and Greenland reflect a largely
lost diversity of root parasites or extinct sister lineages of extant Loranthaceae. These extinct
lineages would then have been replaced, at the earliest, in the middle Oligocene (except for three



992	refugia) in their entire range by their newly evolved aerial parasitic siblings. Using SEM-studied
993	fossil pollen, we can push back the origin(s) of the main Loranthaceae lineages to at least the
994	middle Eocene; a time when important hosts of modern epiphytic Loranthaceae evolved and
995	radiated, and Earth enjoyed a phase of ameliorated climate. The new dating estimates are
996	furthermore relatively stable regarding alternative rooting scenarios for the family.

997

998

1004

Acknowledgements

- Ignacio Escapas and Benjamin Bomfleur are thanked for supplying South American literature,
- 1000 Kanchi Natarajan Gandhi from the IPNI team for clarifying the standard author form for the
- 1001 Indian palynologist Satish Srivastava, and Marco Simeone for providing a compilation of plastid
- substitution rates reported in literature. Alastair Potts and Maxine Smit are acknowledged for
- proof-reading the original submission and final manuscript.

References

- Amico GC, Vidal-Russell R, Garcia MA, Nickrent DL. 2012. Evolutionary history of the South
 American mistletoe *Tripodanthus* (Loranthaceae) using nuclear and plastid markers.

 Systematic Botany 37:218–225.
- Baele G, Lemey P, Bedford T, Rambaut A, Suchard MA, Alekseyenko AV. 2012. xxx.
 Molecular Biology and Evolution 29:2157–2167.
- 1010 Baele G, Li WLS, Drummond AJ, Suchard MA, Lemey P. 2013. xxx. *Molecular Biology and Evolution* 30:239–243.
- Barlow BA. 1990. Biogeographical relationships of Australia and Malesia: Loranthaceae as a model. In: Baas P, Kalkmann K, and Geesink R, eds. *The Plant Diversity of Malesia*. Dortrecht, Boston, London: Kluwer Academic Publishers, 273–292.
- Bartlett AS, Barghoorn ES. 1973. Phytogeographic history of the Isthmus of Panama during the past 12,000 years (a history of vegetation, climate, and sea-level change). In: Graham A, ed. *Vegetation and Vegetational History of Northern Latin America*. Amsterdam: Elsevier Science Publishers.
- Blakey RC. 2008. Gondwana paleogeography from assembly to breakup—A 500 m.y. odyssey.
 In: Fielding CR, Frank TD, and Isbell JL, eds. *Resolving the Late Paleozoic Ice Age in Time and Space*. Boulder: Geological Society of America, 1–28.
- Bouchal JM, Zetter R, Denk T. 2016. Pollen and spores of the uppermost Eocene Florissant Formation, Colorado: a combined light and scanning electron microscopy study. *Grana* 55:179–245.
- Caires CS. 2012. Estudos taxonômicos aprofundados de O*ryctanthus (*Griseb.) Eichler, O*ryctina* Tiegh, e P*usillanthus K*uijt (Loranthaceae) Ph.D. Universidade de Brasília.



- 1027 Chen S-C, Zhang L, Zeng J, She F, Yang H, Mao Y-R, Fu C-X. 2012. Geographic variation of chloroplast DNA in *Platycarya strobilacea* (Juglandaceae). *Journal of Systematics and Evolution* 50:374–385.
- 1030 Cohen KM, Finney SC, Gibbard PL, Fan J-X. 2013 (updated). The ICS International Chronostratigraphic Chart. *Episodes* 36:199–204.
- Dam G, Pedersen GK, Sønderholm M, Midtgaard HH, Larsen LM, H. N-H, Pedersen AK. 2009. Lithostratigraphy of the Cretaceous-Paleocene Nuussuaq Group, Nuussuaq Basin, West Greenland. *Geological Survey of Denmark and Greenland Bulletin* 19:1–171.
- Darriba D, Taboada GL, Doallo R, Posada D. 2012. jModelTest 2: more models, new heuristics and parallel computing. *Nature Methods* 9:772–772.
- del Carmen Zamaloa M, Fernández CA. 2016. Pollen morphology and fossil record of the feathery mistletoe family Misodendraceae. *Grana* 55:278–285.
- Désamoré A, Laenen B, Devos N, Popp M. 2011. Out of Africa: north-westwards Pleistocene expansions of the heather *Erica arborea*. *Journal of Biogeography* 38:164–176.
- Dilcher DL, Lott TA. 2005. A middle Eocene fossil plant assemblage (Power Clay Pit) from western Tennessee. *Bulletin of the Florida Museum of Natural History* 45:1–43.
- Dornburg A, Brandley MC, McGowen MR, Near TJ. 2012. Relaxed clocks and inferences of heterogeneous patterns of nucleotide substitution and divergence time estimates across whales and dolphins (Mammalia: Cetacea). *Molecular Biology and Evolution* 29:721– 736.
- Downey PO. 1998. An inventory of host species for each aerial mistletoe species (Loranthaceae and Viscaceae) in Australia. *Cunninghamia* 5:685–719.
- Drummond AJ, Rambaut A. 2007. BEAST: Bayesian evolutionary analysis by sampling trees. *BMC Evolutionary Biology* 7:214.
- Drummond AJ, Suchard MA, Xie D, Rambaut A. 2012. Bayesian phylogenetics with BEAUti and the BEAST 1.7. *Molecular Biology and Evolution* 29:1969–1973.
- Engelhardt H. 1870. Flora der Braunkohlenformation im Königreich Sachsen. Preisschrift von der Jablonowyn'schen Gesellschaft. Mit einer Mappe enthaltend fünfzehn Tafeln.
 Leipzig: S. Hirzel.
- Eschig M. 1992. Zur Florenentwicklung und Stratigraphie im Mitteloligozän der Kremser Bucht, NÖ, ÖsterreichM.Sc. University of Vienna.
- Ferguson DK, Lee DE, Bannister JM, Zetter R, Jordan GJ, Vavra N, Mildenhall DC. 2009. The taphonomy of a remarkable leaf bed assemblage from the Late Oligocene–Early Miocene Gore Lignite Measures, southern New Zealand. *International Journal of Coal Geology* 83:173–181.
- Feuer SM. 1977. Pollen morphology and evolution in the Santalales sen. str., a parasitic order of flowering plants Ph.D. University of Massachusetts.
- Feuer SM. 1978. Aperture evolution in the genus *Ptychopetalum* Benth. (Olacaceae). *American Journal of Botany* 65:759–763.
- Feuer SM. 1981. Pollen morphology and relationships of the Misodendraceae (Santalales).

 Nordic Journal of Botany 1:731–734.
- Feuer SM, Kuijt J. 1978. Fine structure of mistletoe pollen I. Eremolepidaceae, *Lepidoceras*, and *Tupeia. Canadian Journal of Botany* 56:2853–2864.
- Feuer SM, Kuijt J. 1979. Pollen evolution in the genus *Psittacanthus* Mart. Fine structure of mistletoe pollen II. *Botaniska Notiser* 132:295–309.



- Feuer SM, Kuijt J. 1980. Fine structure of mistletoe pollen III. Large-flowered neotropical Loranthaceae and their Australian relatives. *Annals of the Missouri Botanical Garden* 72:187–212.
- Feuer SM, Kuijt J. 1982. Fine structure of mistletoe pollen IV. Eurasian and Australian *Viscum* L. (Viscaceae). *American Journal of Botany* 69:1–12.
- Feuer SM, Kuijt J. 1985. Fine structure of mistletoe pollen VI. Small-flowered neotropical Loranthaceae. *Annals of the Missouri Botanical Garden* 72:187–212.
- Feuer SM, Kuijt J, Wiens D. 1982. Fine structure of mistletoe pollen V. Madagascan and continental African *Viscum* L. (Viscaceae). *American Journal of Botany* 69:163–187.
- 1081 Garzón-Orduña IJ, Silva-Brandão KL, Willmott KR, Freitas AVL, Brower AVZ. 2015.
 1082 Incompatible ages for clearwing butterflies based on alternative secondary calibrations.
 1083 Systematic Biology 64:752–767.
- Göker M, Grimm GW. 2008. General functions to transform associate data to host data, and their use in phylogenetic inference from sequences with intra-individual variability. *BMC*Evolutionary Biology 8:86.
- Graham A. 1990. Late Tertiary microfossil flora from the Republic of Haiti. *American Journal of Botany* 77:911–926.
- 1089 Gregor H-J. 2005. Pflanzen und Tiere aus den eozänen Braunkohlen des Untertagebaues 1090 Stolzenbach bei Kassel. *Philippia* 12.
- 1091 Gregor H-J, Oschkinis V. 2013. Die eozänen Braunkohleschichten aus dem Untertagebau Stolzenbach bei Kassel (PreußenElektra, Niederhessen) XI. Die tierischen Reste Insekten. *Documenta naturae* 193:51–56.
- Grimm GW, Kapli P, Bomfleur B, McLoughlin S, Renner SS. 2015. Using more than the oldest fossils: Dating Osmundaceae with the fossilized birth-death process. *Systematic Biology* 64:396–405.
- Grimm GW, Renner SS. 2013. Harvesting GenBank for a Betulaceae supermatrix, and a new chronogram for the family. *Botanical Journal of the Linnéan Society* 172:465–477.
- Grimm GW, Renner SS, Stamatakis A, Hemleben V. 2006. A nuclear ribosomal DNA phylogeny of *Acer* inferred with maximum likelihood, splits graphs, and motif analyses of 606 sequences. *Evolutionary Bioinformatics* 2:279-294.
- 1102 Grímsson F, Denk T, Zetter R. 2008. Pollen, fruits, and leaves of *Tetracentron*1103 (Trochodendraceae) from the Cainozoic of Iceland and western North America and their
 1104 palaeobiogeographic implications. *Grana* 47:1–14.
- Grímsson F, Ferguson DK, Zetter R. 2012. Morphological trends in the fossil pollen of *Decodon* and the paleobiogeographic history of the genus. *International Journal of Plant Sciences* 173:297–317.
- Grímsson F, Grimm GW, Zetter R. 2017. Evolution of pollen morphology in Loranthaceae. Grana DOI:10.1080/00173134.2016.1261939.
- 1110 Grímsson F, Grimm GW, Zetter R, Denk T. 2016. Cretaceous and Paleogene Fagaceae from
 1111 North America and Greenland: evidence for a Late Cretaceous split between *Fagus* and
 1112 the remaining Fagaceae. *Acta Palaeobotanica* 56:000–000.
- Grímsson F, Zetter R, Grimm GW, Krarup Pedersen G, Pedersen AK, Denk T. 2015. Fagaceae pollen from the early Cenozoic of West Greenland: revisiting Engler's and Chaney's Arcto-Tertiary hypotheses. *Plant Systematics and Evolution* 301:809–832.



- Grímsson F, Zetter R, Halbritter H, Grimm GW. 2014a. *Aponogeton* pollen from the Cretaceous and Paleogene of North America and West Greenland: Implications for the origin and palaeobiogeography of the genus. *Review of Palaeobotany and Palynology* 200:161–187.
- Grímsson F, Zetter R, Hofmann C-C. 2011. *Lythrum* and *Peplis* from the Late Cretaceous and Cenozoic of North America and Eurasia: New evidence suggesting early diversification within the Lythraceae. *American Journal of Botany* 98:1801–1815.
- Grímsson F, Zetter R, Pedersen GK, Pedersen AK, Denk T. 2014b. Middle Eocene palaeoflora from a resinite-rich coal bed on Hareøn (Qeqertarsuatsiag), West Greenland. 9th European Palaeobotany - Palynology Conference EPPC 2014. Padova. p 86 [abstract].
- Guo S-X. 1979. Late Cretaceous and Early Tertiary floras from the southern Guangdong and Guangxi with their stratigraphic significance [in Chinese]. In: Institute of Vertebrate Palaeontology and Palaeoanthropology, Nanjing Institute of Geology and Palaeontology, and Academia Sinica, eds. *Mesozoic and Cenozoic red beds of South China*. Bejing: Science Press, 223–230.
- Guzmán B, Vargas P. 2010. Unexpected synchronous differentiation in Mediterranean and Canarian *Cistus* (Cistaceae). *Perspectives in Plant Ecology, Evolution and Systematics* 12:163–174.
- Hald N. 1976. Early Tertiary flood basalts from Hareøen and western Nûgssuaq, West Greenland. *Grønlands Geologiske Undersøgelse Bulletin* 120:1–36.
- Hald N. 1977. Lithostratigraphy of the Maligât and Hareøen Formations, West Greenland Basalt Group, on Hareøen and western Nûgssuaq. *Rapport Grønlands Geologiske Undersøgelse* 79:9–16.
- Han R-L, Zhang D-X, Hao G. 2004. Pollen morphology of the Loranthaceae from China. *Acta Phytotaxonomica Sinica* 42:436–456.
- Heath TA, Huelsenbeck JP, Stadler T. 2014. The fossilized birth–death process for coherent calibration of divergence-time estimates. *Proceedings of the National Academy of Sciences* 111:E2957–E2966.
- Heer O. 1883. Flora fossilis arctica 7. Die fossile Flora der Polarländer. Enthaltend: Den zweiten Theil der fossilen Flora Grönlands. Zürich: J. Wurster & Comp.
- Hochuli PA. 1978. Palynologische Untersuchungen im Oligozän und Untermiozän der Zentralen und Westlichen Paratethys. *Beiträge zur Paläontologie Österreichs* 4:1–132.
- Holland B, Moulton V. 2003. Consensus networks: A method for visualising incompatibilities in collections of trees. In: Benson G, and Page R, eds. *Algorithms in Bioinformatics: Third International Workshop, WABI, Budapest, Hungary Proceedings*. Berlin, Heidelberg, Stuttgart: Springer Verlag, 165-176.
- Hottenrott M, Gregor H-J, Oschkinis V. 2010. Die eozäne Braunkohleschichten aus dem Untertagebau Stolzenbach bei Kassel (PreußenElektra, Niederhessen) VII. Die Mikroflora. *Documenta naturae* 181:29–43.
- Huang C, Zhang Y, Bartholomew B. 1999. Fagaceae. In: Wu Z-Y, and Raven PH, eds. *Flora of China 4 Cycadaceae through Fagaceae*. Beijing, St. Louis: Science Press and Missouri Botanical Garden Press.
- Hubert F, Grimm GW, Jousselin E, Berry V, Franc A, Kremer A. 2014. Multiple nuclear genes stabilize the phylogenetic backbone of the genus *Quercus*. *Systematics and Biodiversity* 12:405–423.
- Huelsenbeck JP, Bollback JP, Levine AM. 2002. Inferring the root of a phylogenetic tree.

 Systematic Biology 51:32–43.



- Huson DH, Bryant D. 2006. Application of phylogenetic networks in evolutionary studies. *Molecular Biology and Evolution* 23:254-267.
- Jin J-H, Liao W-B, Wang B-S, Peng S-L. 2002. Palaeodiversification of the environment and plant community of Tertiary in Hainan Island [in Chinese with English abstract]. *Acta Ecologica Sinica* 22:425–432.
- 1167 Kass RE, Raftery AE. 1995. Bayes factors. *Journal of the American Statistical Association* 90:773–795.
- Kmenta M. 2011. Die Mikroflora der untermiozänen Fundstelle Altmittweida, Deutschland M.Sc. M.Sc. University of Vienna.
- 1171 Kmenta M, Zetter R. 2013. Combined LM and SEM study of the upper Oligocene/lower
 1172 Miocene palynoflora from Altmittweida (Saxony): Providing new insights into Cenozoic
 1173 vegetation evolution of Central Europe. *Review of Palaeobotany and Palynology* 195:1–
 1174 18.
- Krutzsch W, Lenk G. 1973. Sporenpaläontologische Untersuchungen im Alttertiär des
 Weißelster-Beckens. I. Die stratigraphisch wichtigen Pollen- und Sporenformen aus dem
 Profil des Tagebaus Profen. Abhandlungen des Zentralen Geologischen Instituts 18:59–
 76.
- 1179 Kuijt J. 1988. Revision of Tristerix (Loranthaceae). Systematic Botany Monographs 19:1–61.
- Kuijt J. 2011. Pulling the skeleton out of the closet: resurrection of *Phthirusa* sensu Martius and consequent revival of *Passovia* (Loranthaceae). *Plant Diversity and Evolution* 129:159–1182 211.
- Larsen LM, Pedersen AK, Tegner C, Duncan RA, Hald N, Larsen JG. 2015. The age of Tertiary volcanic rocks on the West Greenland continental margin: volcanic evolution and event correlation to other parts of the North Atlantic Igneous Province. *Geological Magazine* 153:487–511.
- Lei YZ, Zhang QR, He W, Cao XP. 1992. Tertiary. In: Wang XF, ed. *Geology of Hainan Island* I Stratigraphy and Palaeontology [in Chinese]. Beijing: Geological Publishing House,
 218–266.
- Liu L-F, Qiu H-X. 1993. Pollen morphology of Loranthaceae in China [in Chinese with English abstract]. *Guihaia* 13:235–245.
- Lockwood JD, Aleksić JM, Zou J, Wang J, Liu J, Renner SS. 2013. A new phylogeny for the genus *Picea* from plastid, mitochondrial, and nuclear sequences. *Molecular Phylogenetics and Evolution* 69:717–727.
- Macphail MK, Jordan GJ, Hopf F, Colhoun EA. 2012. When did the mistletoe family
 Loranthaceae become extinct in Tasmania? Review and conjecture. *Terra Australis*34:255–269.
- Maddison WP, Maddison DR. 2011. Mesquite: a modular system for evolutionary analysis. 2.75 ed.
- Maguire B, Wurdack JJ, Huang Y-C. 1974. Pollen grains of some American Olacaceae. *Grana* 1201 14:26–38.
- 1202 Mai DH. 1995. *Tertiäre Vegetationsgeschichte Europas*. Jena, Stuttgart, New York: Gustav 1203 Fischer Verlag.
- Mai DH, Walther H. 1991. Die oligozänen und untermiozänen Floren NW-Sachsens und des
 Bitterfelder Raumes. Abhandlungen des Staatlichen Museum für Mineralogie und
 Geologie Dresden 38:1–230.



- Manchester SR, Grímsson F, Zetter R. 2015. Assessing the fossil record of asterids in the context of our current phylogenetic framework. *Annals of the Missouri Botanical Garden* 100:329–363.
- Marquínez X, Lohmann LG, Salatino MLF, Salatino A, González F. 2009. Generic relationships and dating lineages in Winteraceae based on nuclear (ITS) and plastid (rpS16 and psbA-trnH) sequence data. *Molecular Phylogenetics and Evolution* 53:435–449.
- Massoni J, Couvreur TLP, Sauquet H. 2015. Five major shifts of diversification through the long evolutionary history of Magnoliidae (angiosperms). *BMC Evolutionary Biology* 15:49.
- Muller J. 1981. Fossil pollen records of extant angiosperms. *Botanical Review* 47:1–142.
- Müller S, Salomo K, Salazar J, Naumann J, Jaramillo MA, Neinhuis C, Feild TS, Wanke S.
 2015. Intercontinental long-distance dispersal of Canellaceae from the New to the Old
 World revealed by a nuclear single copy gene and chloroplast loci. *Molecular Phylogenetics and Evolution* 84:205–219.
- 1220 Nickrent DL. 1997 onwards. The Parasitic Plant Connection. Nickrent, D. L.
- Nickrent DL, Malécot V, Vidal-Russell R, Der JP. 2010. A revised classification of Santalales. 1222 Taxon 9:538–558.
- Nixon KC. 1997. Fagaceae. In: Flora of North America Editorial Committee, ed. *Flora of North America North of Mexico*. New York: Oxford University Press, 436-537.
- Norton DA, de Lange PJ. 1999. Host specifity in parasitic mistletoes (Loranthaceae) in New Zealand. *Functional Ecology* 13:552–559.
- Oschkinis V, Gregor H-J. 1992. Paläontologische Funde aus der eozänen Braunkohle des Untertagebaus Stolzenbach (PreußenElektra) in Niederhessen – I. Die Flora. *Documenta* naturae 72:1–31.
- Pälchen W, Walter H. 2011. Geologie von Sachsen I. Geologischer Bau und
 Entwicklungsgeschichte. 2. Auflage. Stuttgart: E. Schweizerbart'sche
 Verlagsbuchhandlung.
- Palmer JD. 1991. Plastid chromosomes: structure and evolution. In: Bogorad L, and Vasil IK, eds. *The molecular biology of plastids*. San Diego: Academic Press, Inc., 5–55.
- Pattengale ND, Masoud A, Bininda-Emonds ORP, Moret BME, Stamatakis A. 2009. How many bootstrap replicates are necessary? In: Batzoglou S, ed. *RECOMB 2009*. Berlin, Heidelberg: Springer-Verlag, 184–200.
- Potter FWJ. 1976. Investigations of angiosperms from the Eocene of southeastern North
 America: Pollen assemblages from Miller Pit, Henry County, Tennessee.

 Palaeontographica, Abteilung B 157:44–96.
- Renner SS, Grimm GW, Kapli P, Denk T. 2016. Species relationships and divergence times in beeches: New insights from the inclusion of 53 young and old fossils in a birth-death clock model. *Philosophical Transactions of the Royal Society B*DOI:10.1098/rstb.2015.0135.
- Renner SS, Grimm GW, Schneeweiss GM, Stuessy TF, Ricklefs RE. 2008. Rooting and dating maples (*Acer*) with an uncorrelated-rates molecular clock: Implications for North American/Asian disjunctions. *Systematic Biology* 57:795-808.
- Roldán FJ, Kuijt J. 2005. A new, red-flowered species of *Tripodanthus* (Loranthaceae) from Columbia. *Novon* 15:207–209.
- 1250 Schmidt AG, Riisager P, Abrahamsen N, Riisager J, Pedersen AK, van der Voo R. 2005.
- Palaeomagnetism of Eocene Talerua Member lavas on Hareøen, West Greenland.
- 1252 Bulletin of the Geological Society of Denmark 52:27–38.



- Smith SA, Beaulieu JM, Donoghue MJ. 2009. An uncorrelated relaxed-clock analysis suggests an earlier origin for flowering plants. *Proceedings of the National Academy of Sciences* 107:5897–5902.
- Smith SA, Donoghue MJ. 2008. Rates of molecular evolution are linked to life history in flowering plants. *Science* 322:86–89.
- Song Z-C, Wang W-M, Huang F. 2004. Fossil pollen records of extant angiosperms in China. *Botanical Review* 70:425–458.
- Spicer RA, Herman AB, Liao W, Spicer TEV, Kodrul TM, Yang J, Jin J. 2014. Cool tropics in
 the Middle Eocene: Evidence from the Changchang Flora, Hainan Island, China.
 Palaeogeography, Palaeoclimatology, Palaeoecology 412:1–16.
- Stamatakis A. 2014. RAxML version 8: a tool for phylogenetic analysis and post-analysis of large phylogenies. *Bioinformatics* 30:1312–1313.
- Standke G. 2008. Tertiär. In: Pälchen W, and Walter H, eds. *Geologie von Sachsen Geologischer Bau und Entwicklungsgeschichte*. Stuttgart: E. Schweizerbart'sche Verlagsbuchhandlung,
 358–419.
- Su H-J, Hu J-M, Anderson FE, Der JP, Nickrent DL. 2015. Phylogenetic relationships of Santalales with insights into the origins of holoparasitic Balanophoraceae. *Taxon* 64:491–506.
- Taylor DW. 1989. Selected palynomorphs from the middle Eocene Claiborne Formation, Tenn. (U.S.A.). *Review of Palaeobotany and Palynology* 58:111–128.
- Thomas N, Bruhl JJ, Ford A, Weston PH. 2014. Molecular dating of Winteraceae reveals a complex biogeographical history involving both ancient Gondwanan vicariance and long-distance dispersal. *Journal of Biogeography* 41:894–904.
- 1276 Tropicos.org. 2016. Tropicos® database. Missouri Botanical Garden.
- Tschudy RH. 1973. Stratigraphic distribution of significant Eocene palynomorphs of the Mississippi embayment. *US Geological Survey Professional Paper* 743-B:B1–B24.
- 1279 Vidal-Russell R, Nickrent DL. 2007. The biogeographic history of Loranthaceae. *Darwiniana* 1280 45:52–54.
- Vidal-Russell R, Nickrent DL. 2008a. Evolutionary relationships in the showy mistletoe family (Loranthaceae). *American Journal of Botany* 95:1015–1029.
- Vidal-Russell R, Nickrent DL. 2008b. The first mistletoes: Origins of aerial parasitism in Santalales. *Molecular Phylogenetics and Evolution* 47:523–537.
- Wang H, Blanchard J, Dilcher DL. 2013. Fruits, seeds, and flowers from the Warman clay pit (middle Eocene Claiborne Group), western Tennessee, USA. *Palaeontologia Electronica* 16:31A.
- Weber L, Weiss A. 1983. Bergbaugeschichte und Geologie der österreichischen
 Braunkohlenvorkommen. Archiv für Lagerstättenforschung der Geologischen
 Bundesanstalt 4:1–317.
- Wikström N, Savolainen V, Chase MW. 2001. Evolution of the angiosperms: Calibrating the family tree. *Proceedings of the Royal Society London: B, Biological Sciences* 268:2211–2220.
- Wilson CA, Calvin CL. 2006. An origin of aerial branch parasitism in the mistletoe family, Loranthaceae. *American Journal of Botany* 93:787–796.
- Wolfe KH, Li W-H, Sharp PM. 1987. Rates of nucleotide substitution vary greatly among plant mitochondrial, chloroplast, and nuclear DNAs. *Proceedings of the National Academy of Sciences, USA* 84:9054–9058.



PeerJ

299	Yao Y-F, Bera S, Ferguson DK, Mosbrugger V, Paudayal KN, Jin J-H, Li C-S. 2009.
300	Reconstruction of paleovegetation and paleoclimate in the Early and Middle Eocene,
301	Hainan Island, China. Climate Change 92:169–189.
302	Zachos JC, Pagani M, Sloan L, Thomas E, Billups K. 2001. Trends, rhythms, and aberrations in
303	global climate 65 Ma to present. Science 292:686-693.
304	Zetter R. 1989. Methodik und Bedeutung einer routinemäßig kombinierten lichtmikroskopischen
305	und rasterelektonenmikroskopischen Untersuchung fossiler Mikrofloren. Courier
306	Forschungsinstitut Senckenberg 109:41–50.
307	Zetter R, Hesse M, Huber KH. 2002. Combined LM, SEM and TEM studies of Late Cretaceous
308	pollen and spores from Gmünd, Lower Austria. Stapfia 80:201–230.
309	



1311	Text to Figures and Tables
1312	Table 1. Information on sample sites.
1313	
1314	Table 2. Results of the clock-rooting analyses.
1315	
1316	Table 3. Results of the dating analyses using the reduced taxon data set and different rooting
1317	scenarios.
1318	
1319	Table 4. Estimated substitution rates (per million years) for each of the used genetic markers,
1320	under the four tested topological hypothesis (rooting scenarios 1–3, and scenario 4 constraining
1321	the topology of Su et al. 2015)
1322	
1323	Table 5. Ranking of the four tested topological configurations (three rooting scenarios, and
1324	scenario 4 constraining the topology of Su et al. 2015) based on marginal likelihood estimates
1325	(MLE) and Bayes factors (BF), calculated using two approaches, stepping-stone and path-
1326	sampling, implemented in BEAST (Baele et al. 2012; Baele et al. 2013)
1327	
1328	Figure 1. LM micrographs (polar views) of all fossil Loranthaceae morphotypes. (A) Miller
1329	Clay Pit MT1. (B) Miller Clay Pit MT1. (C) Miller Clay Pit MT2. (D) Miller Clay Pit MT3.
1330	(E) Aamarutissaa MT. (F) Stolzenbach MT. (G) Profen MT1. (H) Profen MT1. (I) Profen
1331	MT2. (J) Profen MT2. (K) Profen MT3. (L) Profen MT4. (M) Profen MT4. (N) Profen MT4.
1332	(O) Profen MT4. (P) Profen MT5. (Q) Profen MT5. (R) Changchang MT. (S) Changchang
1333	MT. (T) Theiss MT. (U) Theiss MT. (V) Theiss MT. (W) Theiss MT. (X) Theiss MT. (Y)
1334	Altmittweida MT. (Z) Altmittweida MT. (Ä) Altmittweida MT.
1335	
1336	Figure 2. SEM micrographs of fossil Loranthaceae pollen similar to/intermediate between root
1337	parasites and Lorantheae and comparable extant pollen. (A–D) Polar views of fossil pollen.
1338	(E-G) Polar views of extant pollen. (H-J) Close-ups of sculpturing in area of mesocolpium
1339	and along margo in fossil pollen. (K-M) Close-ups of sculpturing in area of mesocolpium and
1340	along margo in extant pollen (A. H) Miller Clay Pit MT1 (B. I) Stolzenbach MT (C. I)



```
1341
          Profen MT1. (D) Theiss MT. (E, K) Nuytsia floribunda. (F, L) Gaiadendron punctatum. (G,
1342
          M) Muellerina eucalyptoides. Scale bars: (A–M) = 1 µm.
1343
1344
       Figure 3. SEM micrographs of fossil Loranthaceae pollen with affinity to Tripodanthus and
1345
          extant pollen of the genus. (A–D) Polar views of fossil pollen. (E, F) Polar views of extant
1346
          pollen. (G–J) Close-ups of sculpturing in area of mesocolpium and along margo in fossil
1347
          pollen. (K, L) Close-ups of sculpturing in area of mesocolpium and along margo in extant
1348
          pollen. (A, G) Miller Clay Pit MT2. (B, C, H, I) Miller Clay Pit MT3. (D, J) Aamaruutissaa
          MT. (E, F, K, L) Tripodanthus acutifolius. Scale bars: (A-F) = 10 \mu m, (G-L) = 1 \mu m.
1349
1350
1351
       Figure 4. SEM micrographs of fossil Loranthaceae pollen with affinity to Elytrantheae and
          extant representatives. (A–F) Polar views of fossil pollen. (G-I) Polar views of extant pollen.
1352
1353
          (A) Profen MT2. (B) Profen MT2. (C) Profen MT3. (D) Profen MT4. (E) Profen MT4. (F).
1354
          Profen MT5. (G) Peraxilla tetrapetala. (H) Amylotheca sp. (I) Ligaria cuneifolia. Scale bar:
1355
          (A-I) = 10 \mu m.
1356
1357
       Figure 5. SEM micrographs of fossil Loranthaceae pollen with affinity to Elytrantheae and
1358
          extant representatives. (A–E) Close-ups of sculpturing in area of mesocolpium and along
1359
          margo in fossil pollen. (F–H) Close-ups of sculpturing in area of mesocolpium and along
1360
          margo in extant pollen. (A) Profen MT2. (B) Profen MT2. (C) Profen MT3. (D) Profen MT4.
1361
          (E) Profen MT5. (F) Peraxilla tetrapetala. (G) Amylotheca sp. (H) Ligaria cuneifolia. Scale
1362
          bar: (A-H) = 1 \mu m.
1363
1364
       Figure 6. SEM micrographs of fossil Loranthaceae pollen with affinity to crown group
1365
          Lorantheae and comparable extant pollen. (A–D) Polar views of fossil pollen. (E–G) Polar
1366
          views of extant pollen. (H–J) Close-ups of sculpturing in area of mesocolpium and along
1367
          margo in fossil pollen. (K–M) Close-ups of sculpturing in area of mesocolpium and along
1368
          margo in extant pollen. (A, B, H, I) Changchang MT. (C, D, J) Altmittweida MT. (E, K)
1369
          Amyema gibberula. (F, L) Helixanthera kirkii. (G, M) Taxillus caloreas. Scale bars: (A-G) =
1370
          10 \mu m, (H-M) = 1 \mu m.
1371
```





1372	Figure 7. Plastid and nuclear species trees for the complete taxon set. No high-supported conflict
1373	is found; both datasets recognise the same main clades, while failing to resolve most of the
1374	deeper inter-clade relationships. Particularly, the phylogenetic position of tribes/subtribes with
1375	few, often monotypic, genera (root parasitic Nuytsieae, Gaiadendreae, aerial parasitic
1376	Ligarinae, Notantherinae, and Tupeinae) is essentially unresolved. Local differences in the
1377	topologies and odd placements are often related to species with large amount of missing data.
1378	Stippled terminal lines have been reduced by factor 2.
1379	
1380	Figure 8. Lineage-through-time plots for Loranthaceae as inferred based on three different
1381	rooting scenarios or enforcing the topology of Su et al. (2015; scenario 4). Background shows
1382	the stable-isotope-based (marine sediments) global temperature curve with main climatic
1383	events annotated at the bottom (after Zachos et al. 2001). Increased diversification of
1384	Loranthaceae is inferred for time-scales when the global mean temperature was at least $\sim 5^{\circ}$ C
1385	higher than today (middle to late Eocene; late Oligocene to mid-Miocene).
1386	
1387	Figure 9. A dated phylogeny of Loranthaceae using the pollen-informed root (rooting scenario
1388	3). The chronogram is based on a concatenated data set including two nuclear ribosomal RNA
1389	genes (18S and 25S rDNA), two coding plastid genes (rbcL, matK) and the trnLLF region.
1390	The taxon set has been reduced to species with sufficient data, i.e. data covering all included
1391	gene regions. Node heights (divergence ages) are medians, grey bars indicate the 95%-
1392	highest-posterior-density intervals; labels at branches indicate posterior probabilities for those
1393	branches that did not receive unambiguous support. Triangular doodles represent pollen used
1394	as age priors for the according nodes: green - Central Europe; red - North America (including
1395	Greenland); yellow – East Asia. Abbreviations: ECO = Eocene warm phase; MCO = Miocene
1396	warm phase (see Fig. 8)
1397	
1398	Figure 10. Global distribution of Loranthaceae in the Paleogene, evidenced based on
1399	unequivocal palynological records (see File S4). (A) Eocene. (B) Oligocene. Maps are
1400	Mollweide views, projected through the prime meridian (Blakey 2008; Global DVD $\ensuremath{\mathbb{C}}$ 2011
1401	Colorado Plateau Geosystems Inc.)
1402	





1403	Figure 11. Global distribution of Loranthaceae in the Neogene, evidenced based on unequivocal
1404	palynological records (see File S4). (A) Miocene. (B) Pliocene to recent. Maps are Mollweide
1405	views, projected through the prime meridian (Blakey 2008; Global DVD © 2011 Colorado
1406	Plateau Geosystems Inc.)



LM micrographs (polar views) of all fossil Loranthaceae morphotypes

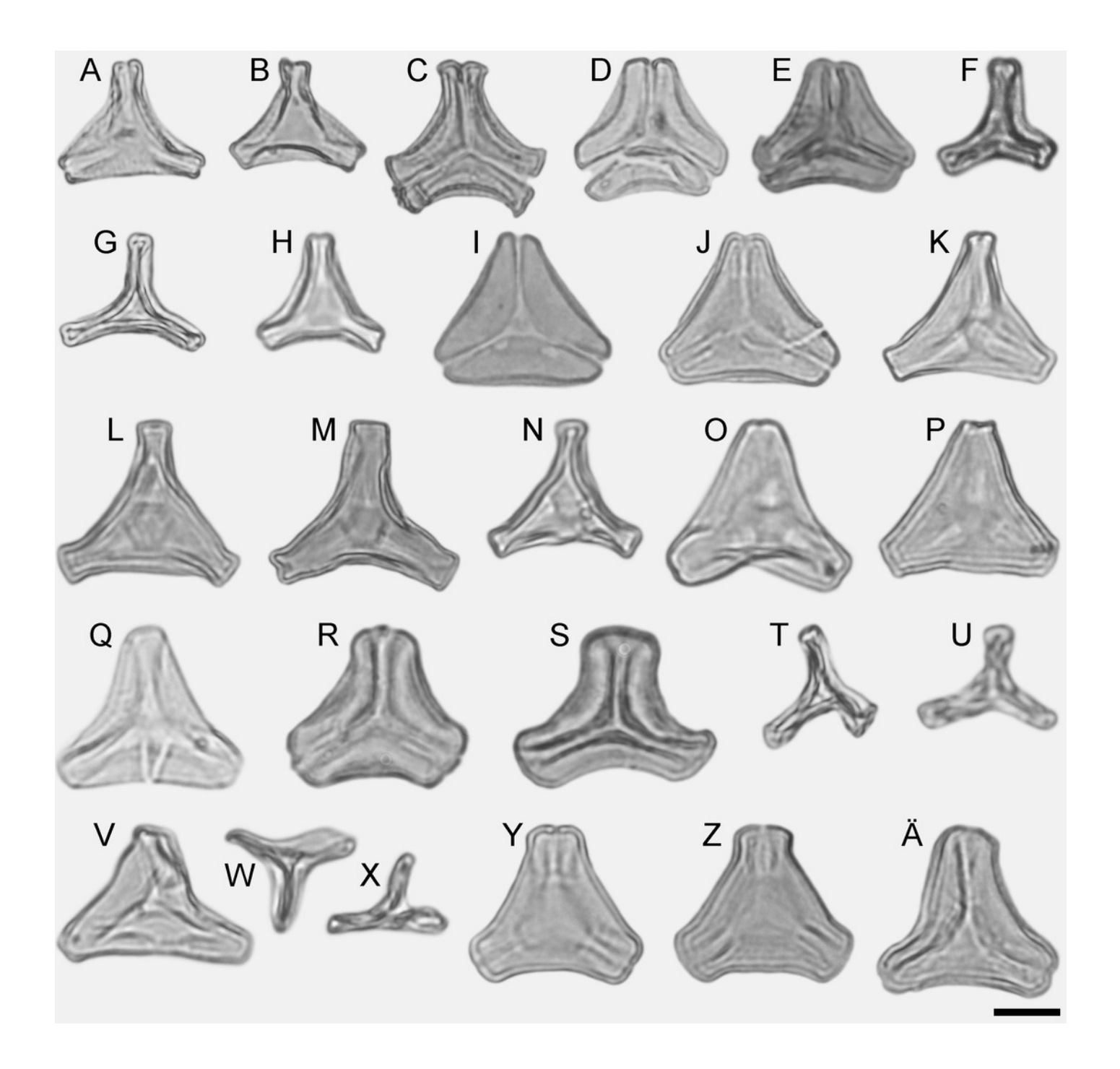
- (A) Miller Clay Pit MT1. (B) Miller Clay Pit MT1. (C) Miller Clay Pit MT2. (D) Miller Clay Pit MT3.
- (E) Aamarutissaa MT. (F) Stolzenbach MT. (G) Profen MT1. (H) Profen MT1. (I) Profen MT2. (J)

Profen MT2. (K) Profen MT3. (L) Profen MT4. (M) Profen MT4. (N) Profen MT4. (O) Profen MT4.

(P) Profen MT5. (Q) Profen MT5. (R) Changchang MT. (S) Changchang MT. (T) Theiss MT. (U)

Theiss MT. (V) Theiss MT. (W) Theiss MT. (X) Theiss MT. (Y) Altmittweida MT. (Z) Altmittweida

MT. (Ä) Altmittweida MT.

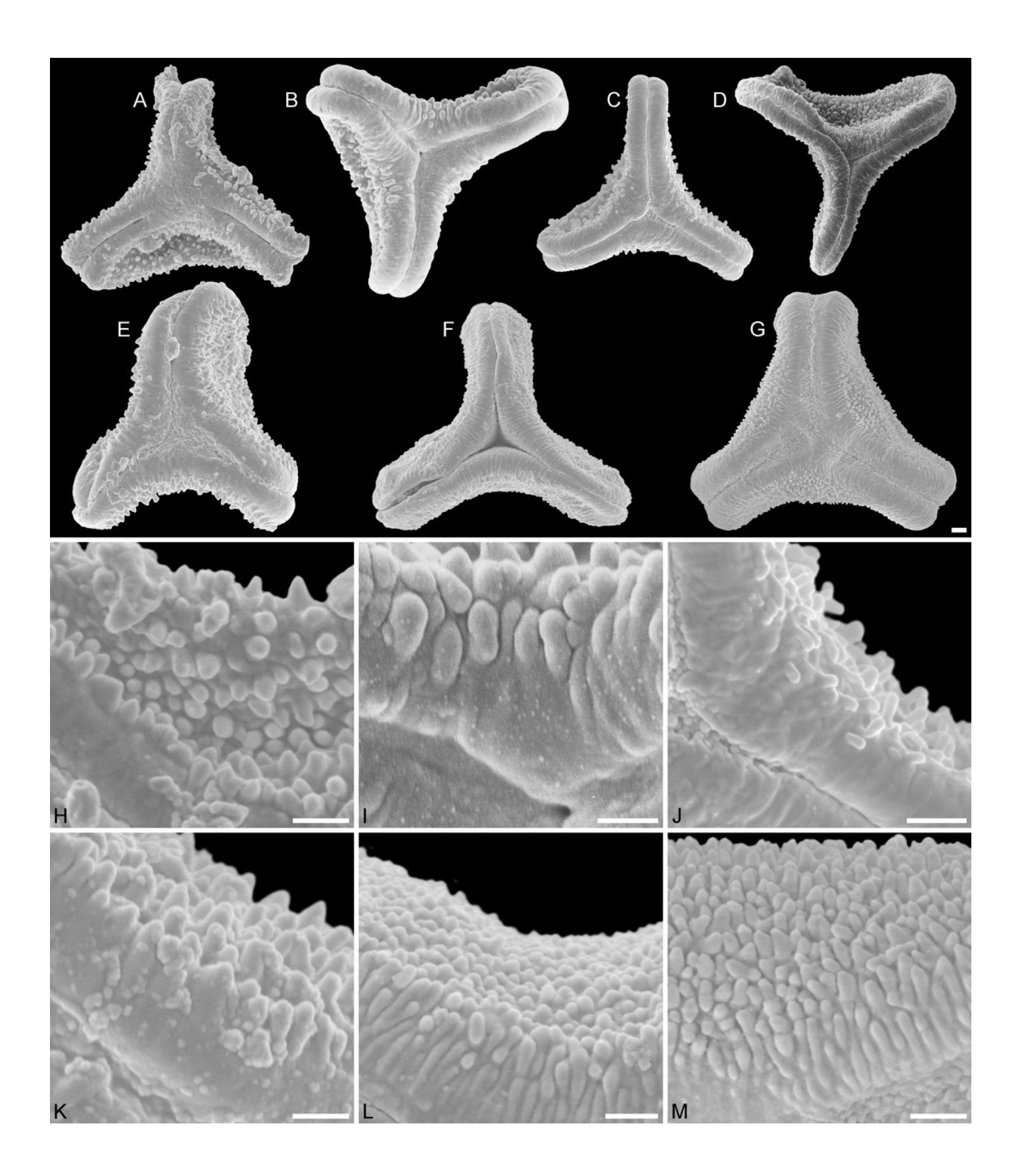




SEM micrographs of fossil Loranthaceae pollen similar to/intermediate between root parasites and Lorantheae and comparable extant pollen

(A–D) Polar views of fossil pollen. (E–G) Polar views of extant pollen. (H–J) Close-ups of sculpturing in area of mesocolpium and along margo in fossil pollen. (K–M) Close-ups of sculpturing in area of mesocolpium and along margo in extant pollen. (A, H) Miller Clay Pit MT1. (B, I) Stolzenbach MT. (C, J) Profen MT1. (D) Theiss MT. (E, K) *Nuytsia floribunda*. (F, L) *Gaiadendron punctatum*. (G, M) *Muellerina eucalyptoides*. Scale bars: (A–M) = 1 μm.

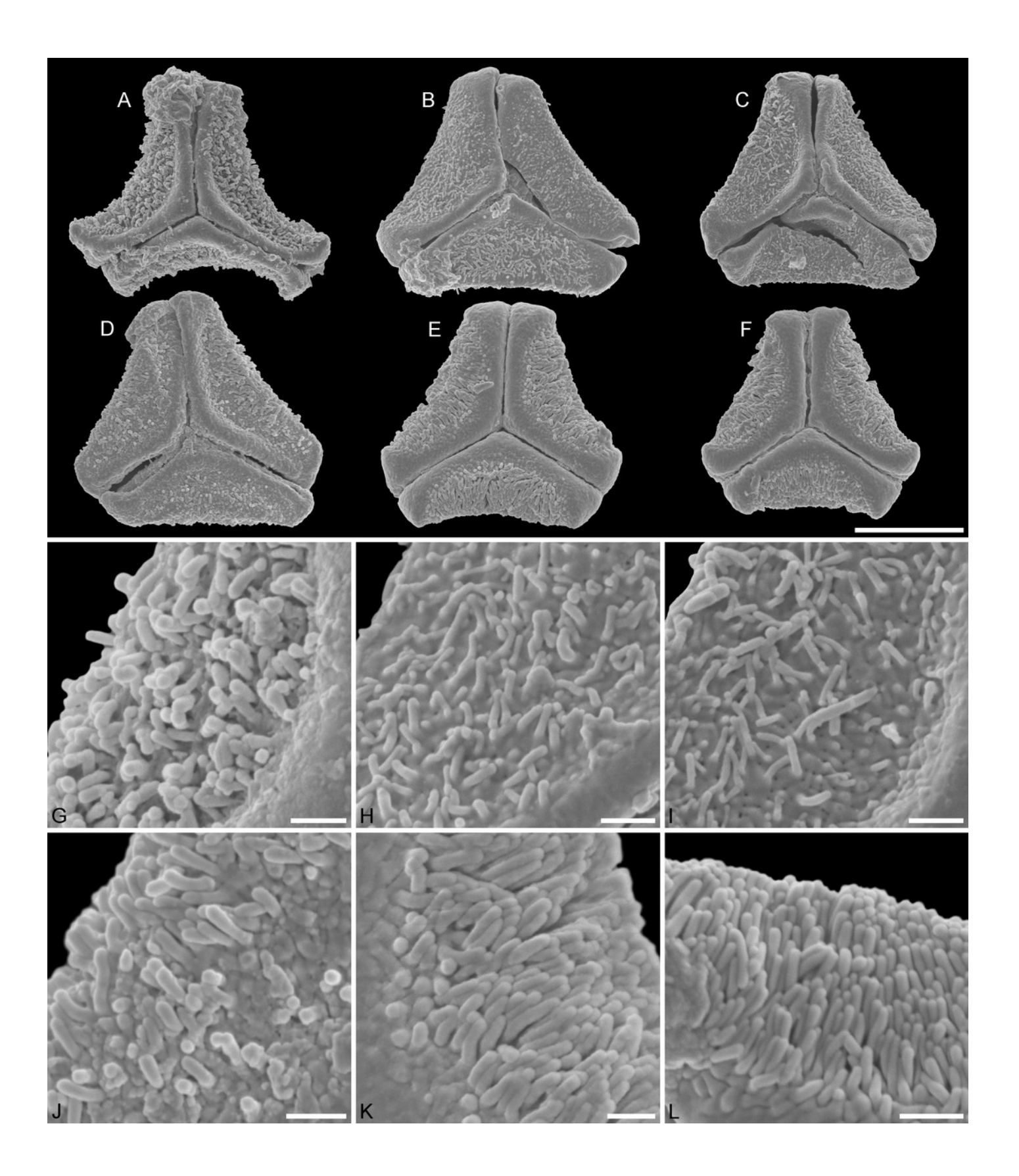
*Note: Auto Gamma Correction was used for the image. This only affects the reviewing manuscript. See original source image if needed for review.





SEM micrographs of fossil Loranthaceae pollen with affinity to *Tripodanthus* and extant pollen of the genus

(A–D) Polar views of fossil pollen. (E, F) Polar views of extant pollen. (G–J) Close-ups of sculpturing in area of mesocolpium and along margo in fossil pollen. (K, L) Close-ups of sculpturing in area of mesocolpium and along margo in extant pollen. (A, G) Miller Clay Pit MT2. (B, C, H, I) Miller Clay Pit MT3. (D, J) Aamaruutissaa MT. (E, F, K, L) *Tripodanthus acutifolius*. Scale bars: (A–F) = $10 \mu m$, (G-L) = $1 \mu m$.

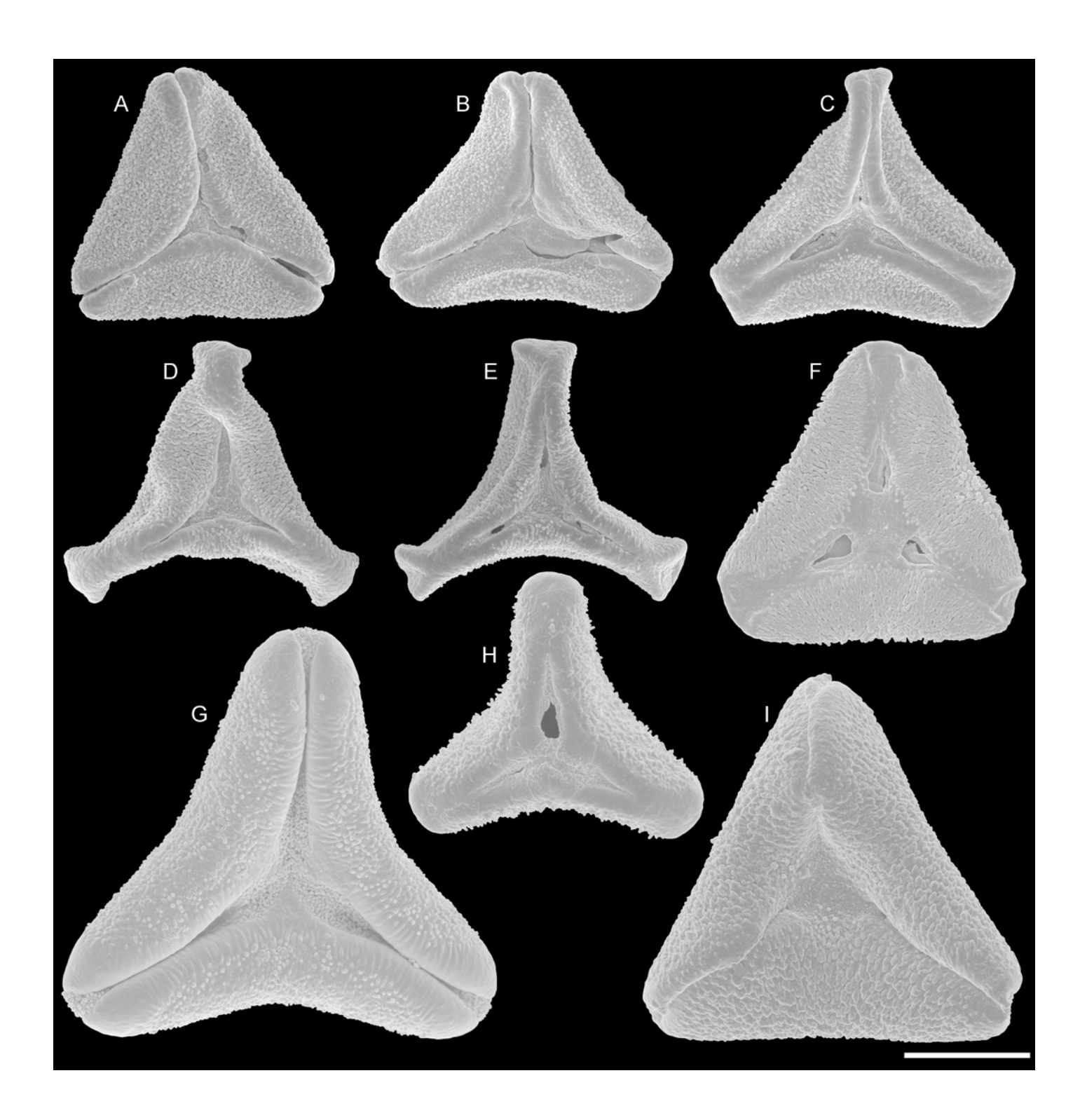




SEM micrographs of fossil Loranthaceae pollen with affinity to Elytrantheae and extant representatives

(A–F) Polar views of fossil pollen. (G-I) Polar views of extant pollen. (A) Profen MT2. (B) Profen MT2. (C) Profen MT3. (D) Profen MT4. (E) Profen MT4. (F). Profen MT5. (G) *Peraxilla* tetrapetala. (H) *Amylotheca* sp. (I) *Ligaria cuneifolia*. Scale bar: (A–I) = 10 μ m.

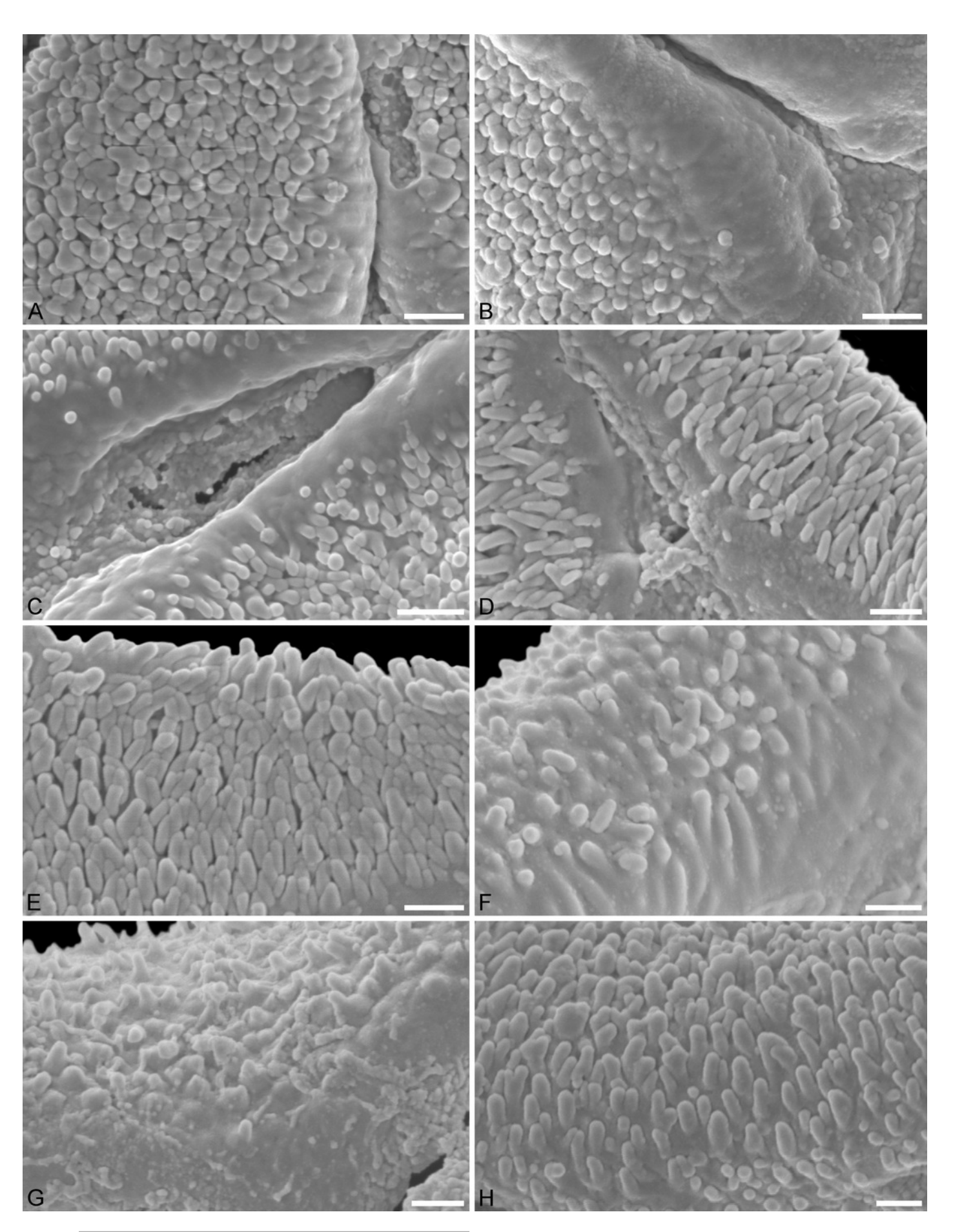
*Note: Auto Gamma Correction was used for the image. This only affects the reviewing manuscript. See original source image if needed for review.





SEM micrographs of fossil Loranthaceae pollen with affinity to Elytrantheae and extant representatives

(A–E) Close-ups of sculpturing in area of mesocolpium and along margo in fossil pollen. (F–H) Close-ups of sculpturing in area of mesocolpium and along margo in extant pollen. (A) Profen MT2. (B) Profen MT2. (C) Profen MT3. (D) Profen MT4. (E) Profen MT5. (F) Peraxilla tetrapetala. (G) Amylotheca sp. (H) Ligaria cuneifolia. Scale bar: (A-H) = 1 μ m.

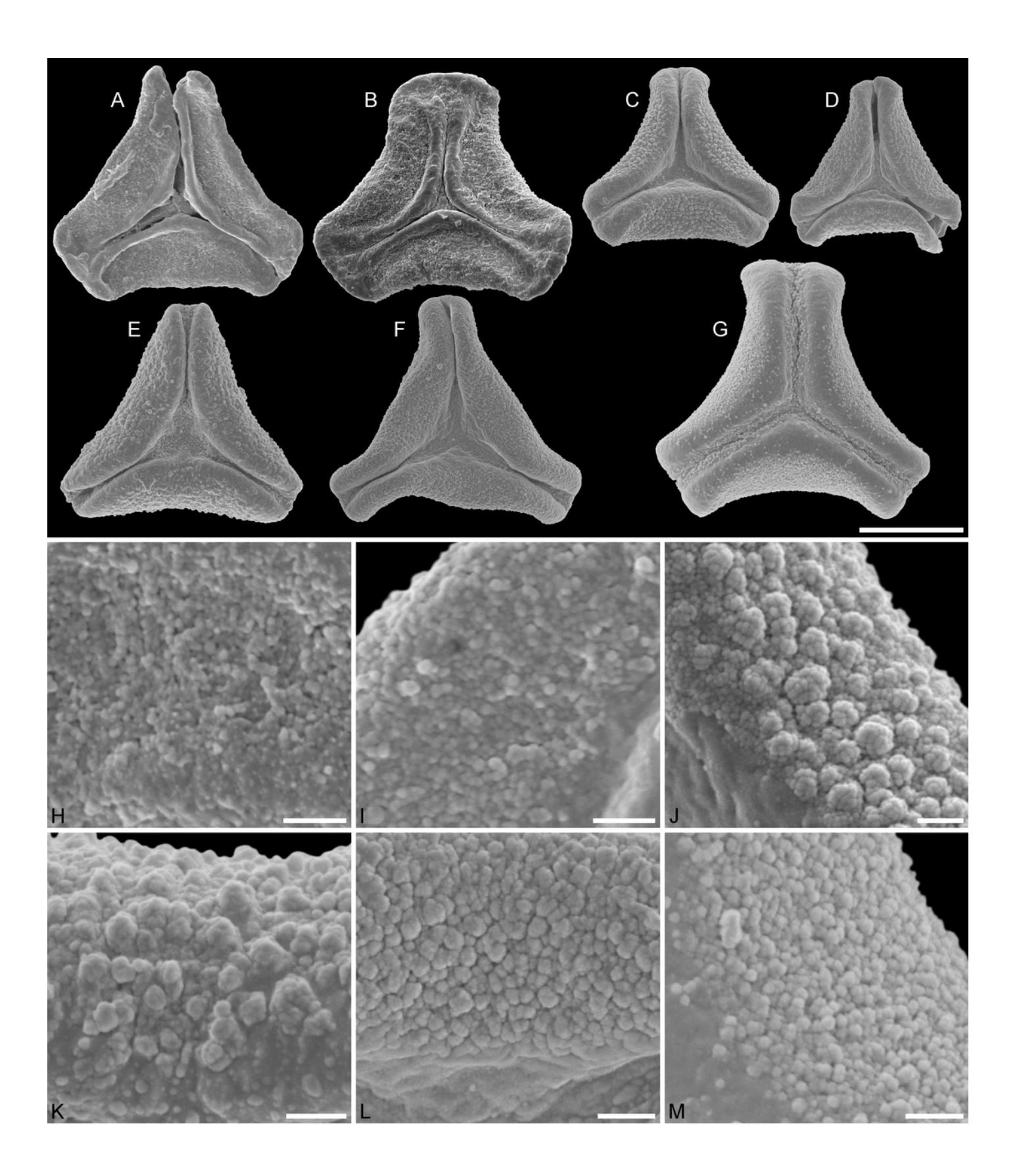


PeerJ reviewing PDF | (2016:12:15035:1:0:NEW 20 Apr 2017)



SEM micrographs of fossil Loranthaceae pollen with affinity to crown group Lorantheae and comparable extant pollen

(A–D) Polar views of fossil pollen. (E–G) Polar views of extant pollen. (H–J) Close-ups of sculpturing in area of mesocolpium and along margo in fossil pollen. (K–M) Close-ups of sculpturing in area of mesocolpium and along margo in extant pollen. (A, B, H, I) Changchang MT. (C, D, J) Altmittweida MT. (E, K) *Amyema gibberula*. (F, L) *Helixanthera kirkii*. (G, M) *Taxillus caloreas*. Scale bars: (A-G) = $10 \mu m$, (H–M) = $1 \mu m$





Plastid and nuclear species trees for the complete taxon set

No high-supported conflict is found; both datasets recognise the same main clades, while failing to resolve most of the deeper inter-clade relationships. Particularly, the phylogenetic position of tribes/subtribes with few, often monotypic, genera (root parasitic Nuytsieae, Gaiadendreae, aerial parasitic Ligarinae, Notantherinae, and Tupeinae) is essentially unresolved. Local differences in the topologies and odd placements are often related to species with large amount of missing data. Stippled terminal lines have been reduced by factor 2.

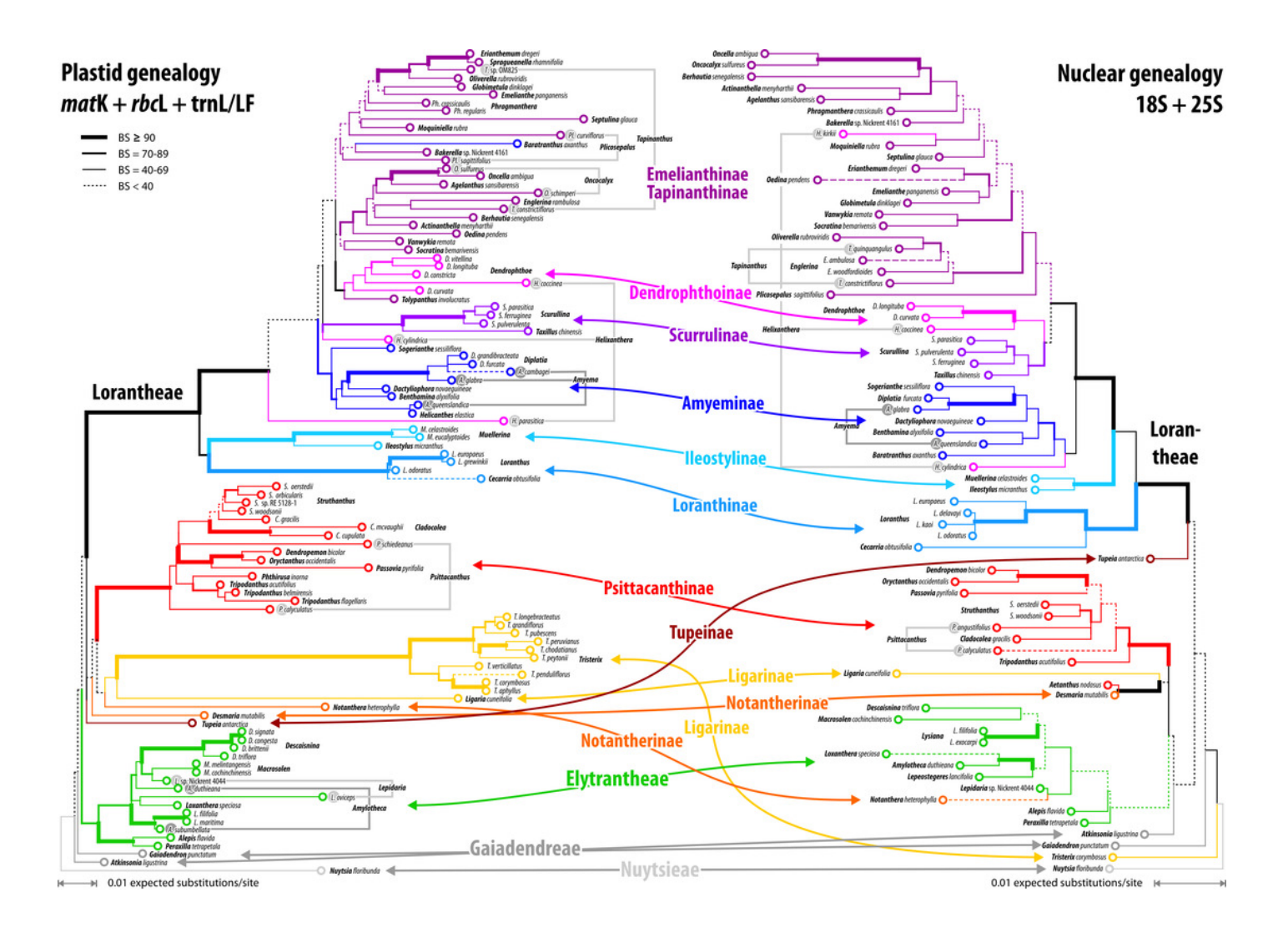




Figure 8(on next page)

Lineage-through-time plots for Loranthaceae as inferred based on three different rooting scenarios or enforcing the topology of Su et al. (2015; scenario 4)

Background shows the stable-isotope-based (marine sediments) global temperature curve with main climatic events annotated at the bottom (after Zachos et al. 2001). Increased diversification of Loranthaceae is inferred for time-scales when the global mean temperature was at least \sim 5° C higher than today (middle to late Eocene; late Oligocene to mid-Miocene).

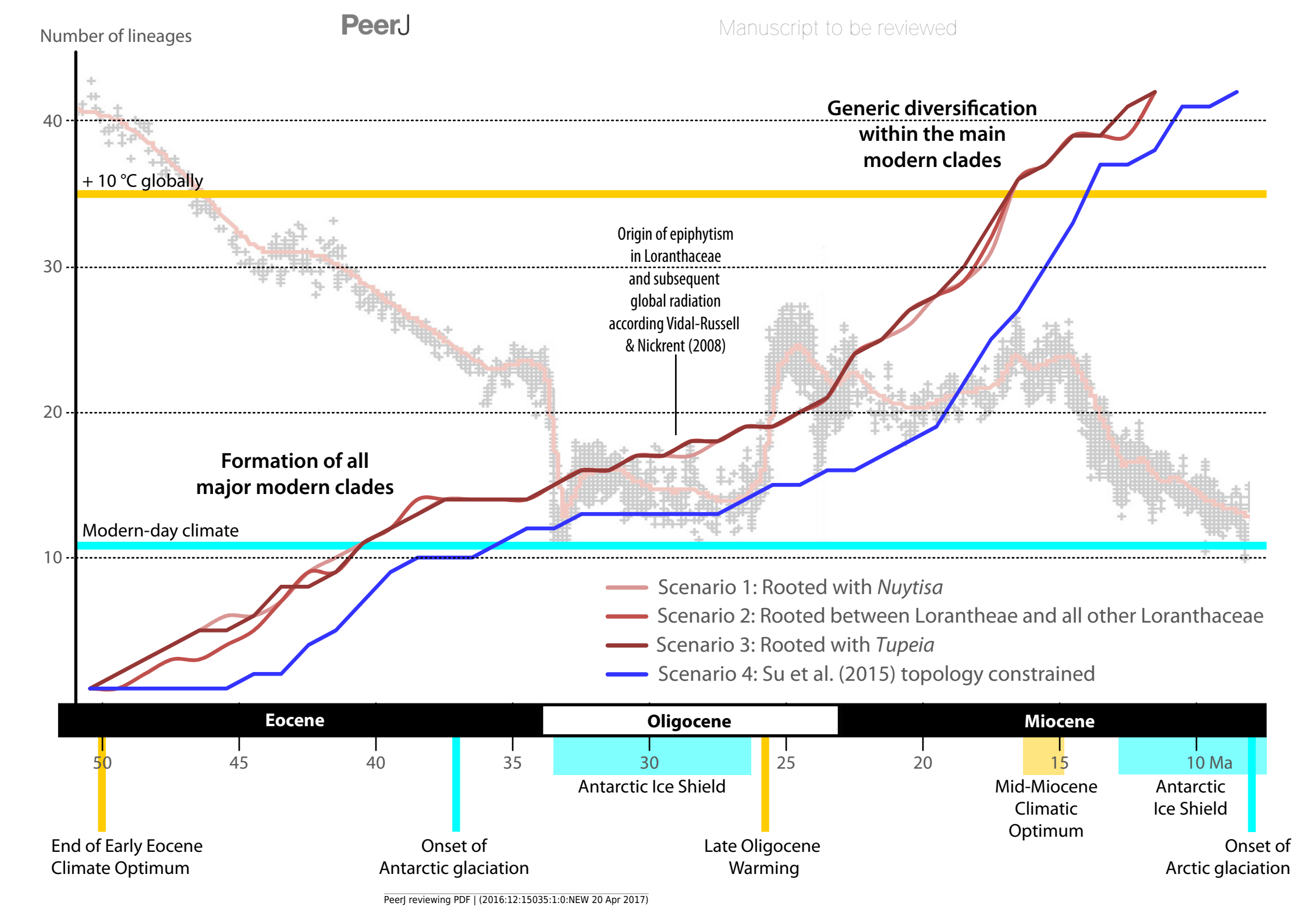




Figure 9(on next page)

A dated phylogeny of Loranthaceae using the pollen-informed root (rooting scenario 3)

The chronogram is based on a concatenated data set including two nuclear ribosomal RNA genes (18S and 25S rDNA), two coding plastid genes (*rbc*L, *mat*K) and the trnLLF region. The taxon set has been reduced to species with sufficient data, i.e. data covering all included gene regions. Node heights (divergence ages) are medians, grey bars indicate the 95%-highest-posterior-density intervals; labels at branches indicate posterior probabilities for those branches that did not receive unambiguous support. Triangular doodles represent pollen used as age priors for the according nodes: green – Central Europe; red – North America (including Greenland); yellow – East Asia. Abbreviations: ECO = Eocene warm phase; MCO = Miocene warm phase (see Fig. 8)

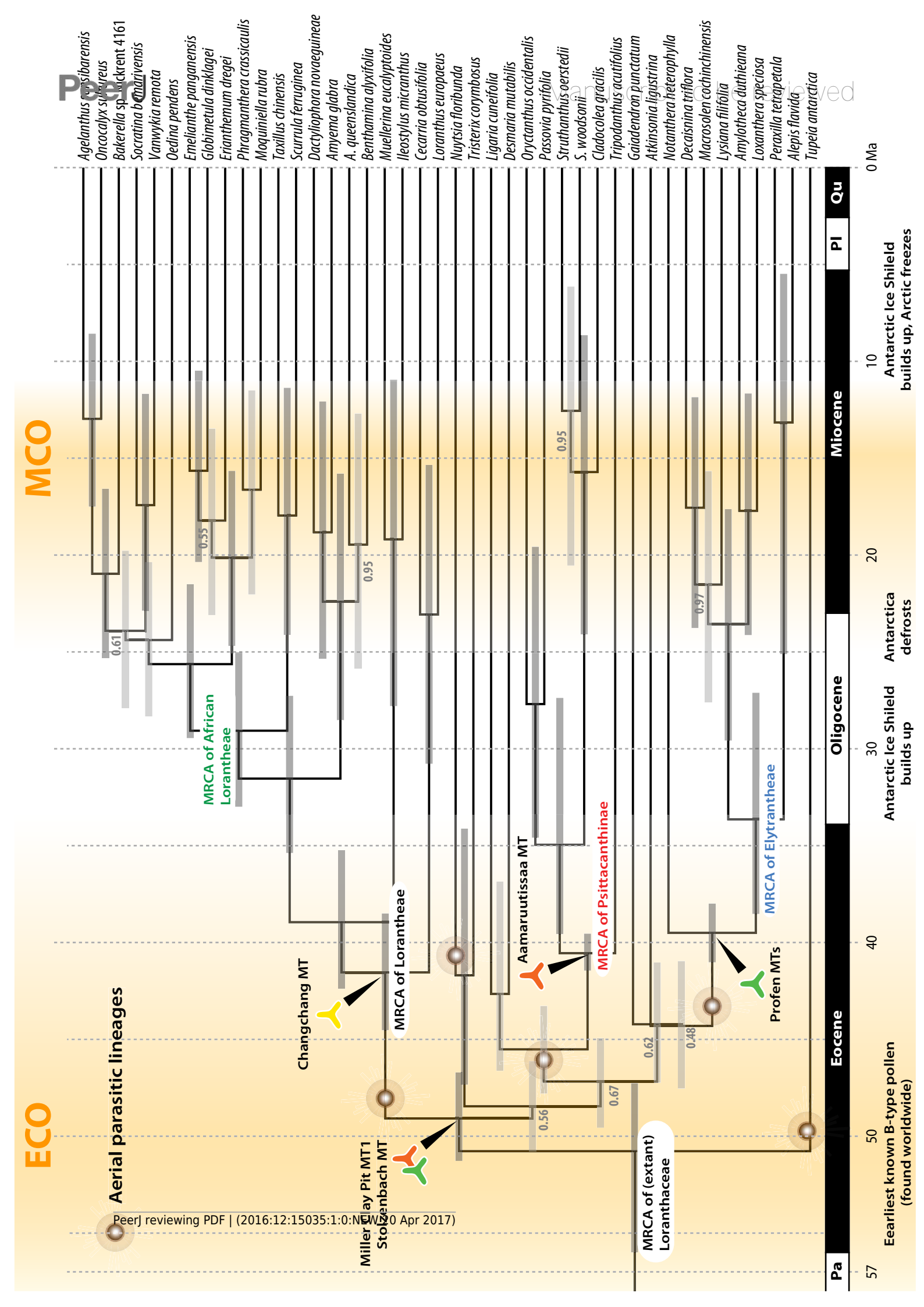




Figure 10(on next page)

Global distribution of Loranthaceae in the Paleogene, evidenced based on unequivocal palynological records

(A) Eocene. (B) Oligocene. Maps are Mollweide views, projected through the prime meridian (Blakey 2008)

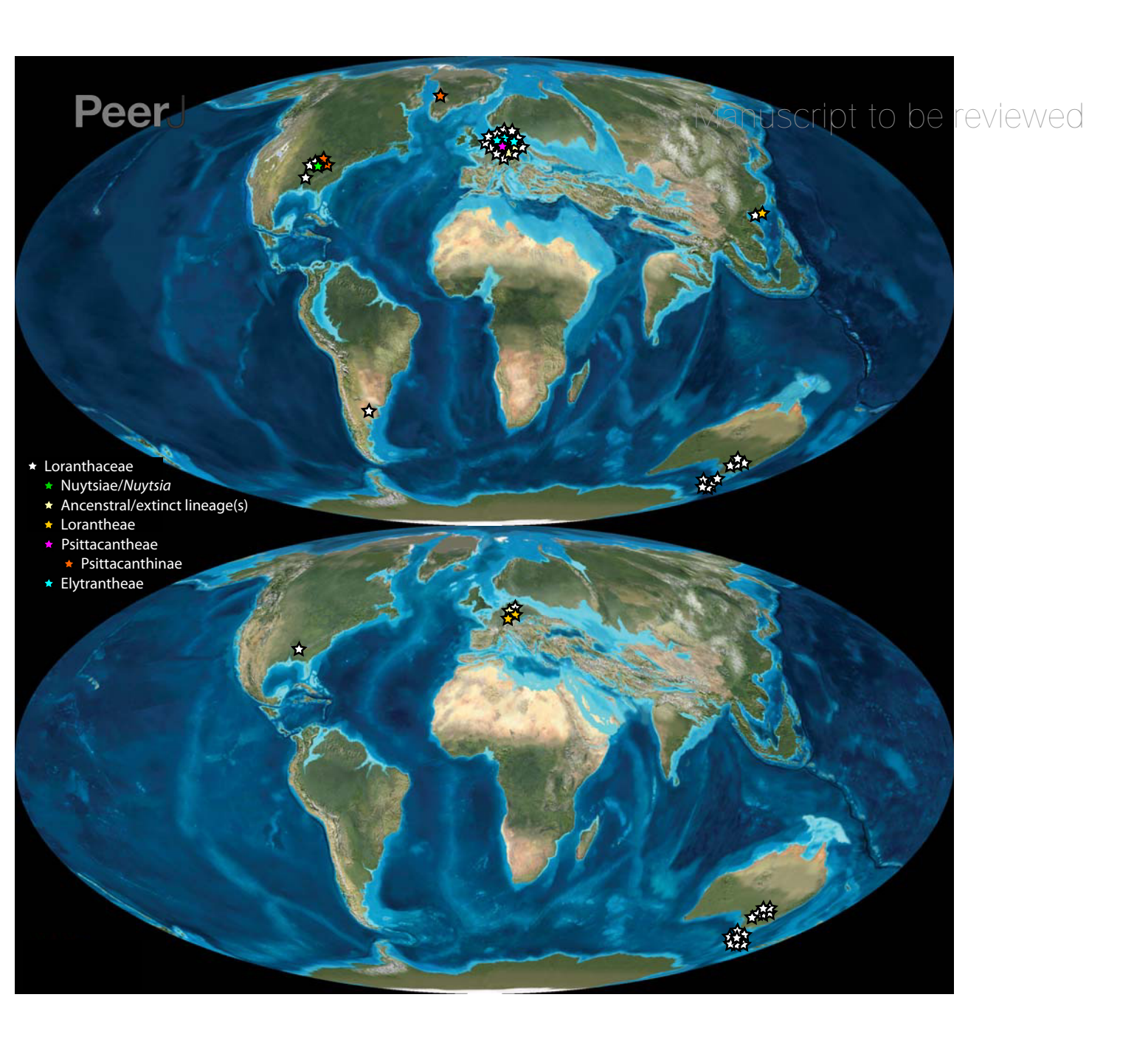




Figure 11(on next page)

Global distribution of Loranthaceae in the Neogene, evidenced based on unequivocal palynological records

(A) Miocene. (B) Pliocene to recent. Maps are Mollweide views, projected through the prime meridian (Blakey 2008)

PeerJ

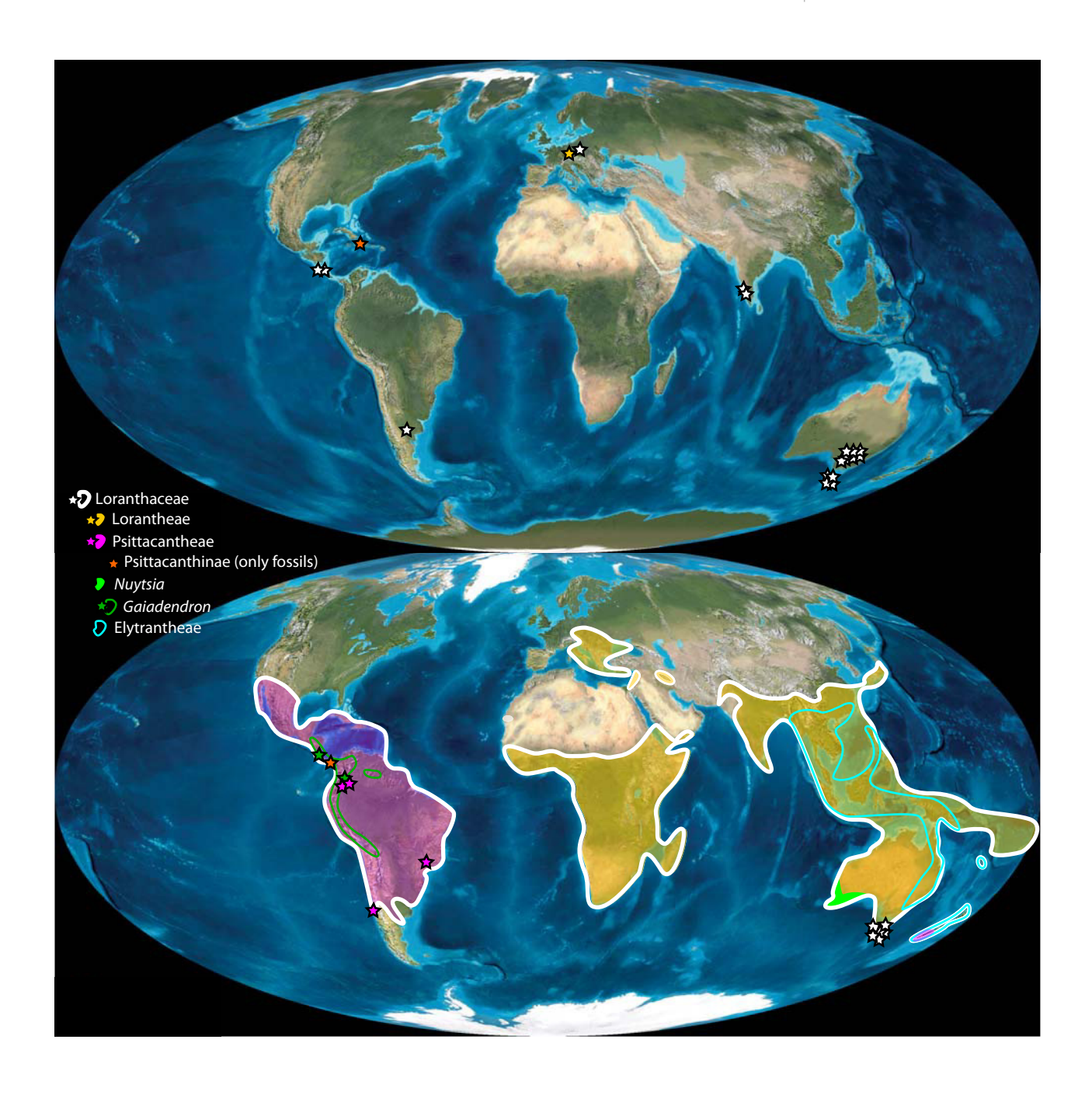




Table 1(on next page)

Information on sample sites

	Miller Clay Pit MT1-MT3	Aamaruutissaa MT	Stolzenbach MT	Profen MT1-MT5	Changchang MT	Theiss MT	Altmittweida MT	
Location	Miller Clay Pit, Henry County, Tennessee, United States	Aamaruutissaa, southeast Hareøen Island, western Greenland	Stolzenbach underground coalmine, Kassel, Germany	Profen opencast mine, close to Leipzig, Germany	Changchang Basin, close to Jiazi Town, Qiongshan County, Hainan, China	Theiss, borehole southeast of Krems, Lower Austria	Altmittweida, Saxony, Germany	
Latitude and longitude (ca.)	36°13′N, 88°27′W	70°24′N, 54°41′W	51°0′N, 9°17′E	51°09′N, 12°11′E	19°38′N, 110°27′E	48°23′N, 15°41′E	50°58′N, 12°55′E	
Lithostratigraphy	Claiborne Group	Hareøen Formation	Borkener coal measures	Profen Formation	Changchang Formation	Melker Series	Cottbus/Sprember g Formations	
Epoch*	Lutetian	Late Lutetian-early Bartonian	Lutetian	Bartonian	Lutetian-Bartonian	Rupelian	Chattian to Aquitanian	
Age (Ma)*	47.8–41.2*	42–40 [absolute dating]	47.8–41.2*	41.2–38*	47.8–37.8*	33.9–28.1*	28.1–20.44*	
According to	Litho- and biostratigraphy	Chrono-, litho- and biostratigraphy	Litho- and biostratigraphy	Litho- and biostratigraphy	Litho- and biostratigraphy	Litho- and biostratigraphy	Litho- and biostratigraphy	
Notes on palynofloras	Dominated by angiosperms; rich in Fagaceae, Juglandaceae, Sapotaceae, Anarcardiaceae, Olacaceae, Cannabaceae, and Altingiaceae	Diverse spore and pollen flora; rich in Cupressaceae and angiosperms; <i>Fagus</i> , <i>Quercus</i> and Castaneoideae pollen abundant	Dominated by angiosperms; rich in Ericaceae, Fagaceae, Hamamelidaceae, Altingiaceae, Combretaceae, Burseraceae, Icacinaceae, Juglandaceae, Lecythidiaceae, and Sapotaceae	Dominated by angiosperms; rich in Anacardiaceae, Araceae, Arecaceae, Fagaceae, Sapotaceae, Symplocaceae, and Combretaceae	Diverse in angiosperms; rich in Fagaceae pollen, especially <i>Quercus</i> and Castaneoideae	Dominated by angiosperms, rich in Fagaceae, Sapotaceae, Juglandaceae, Vitaceae, Malvaceae, Symplocaceae, Cornaceae, Oleaceae, and Arecaceae	Diverse in angiosperms; rich in Juglandaceae and Fagaceae genera	
For further info on the geological background, stratigraphy [S], paleoenvironment , paleoclimate, and plant fossils [P]	Tschudy (1973[P]); Potter (1976[P]); Taylor (1989[P]); Dilcher & Lott (2005[P/S]); Wang, Blanchard & Dilcher (2013[P])	Heer (1883[P]); Hald (1976, 1977[S]); Schmidt et al. (2005[S]); Dam et al. (2009[S]); Grímsson et al. (2014, 2015); Larsen et al. (2015[S]); Manchester, Grímsson & Zetter (2015[P])	Oschkinis & Gregor (1992[P/S]); Gregor (2005[P]); Hottenrott, Gregor & Oschkinis (2010[P]); Gregor & Oschkinis (2013[P]); Manchester, Grimsson & Zetter (2015[P])	Krutzsch & Lenk (1973[P/S]); Pälchen & Walter (2011[S]); Manchester, Grímsson & Zetter (2015[P])	Guo (1979[P]); Lei et al. (1992[P]); Jin et al. (2002[P]); Yao et al. (2009[P]); Spicer et al. (2014[S/P])	Hochuli (1978[P]); Weber & Weiss (1983[S]); Eschig (1992[P/S]); Grímsson, Ferguson & Zetter (2012[P])	Engelhardt (1870[P]); Mai & Walther (1991[P]); Standke (2008[S]); Kmenta (2011[P]); Kmenta & Zetter (2013[P])	

^{*} Following Cohen et al. (2013, onwards)



Table 2(on next page)

Results of the clock-rooting analyses



Species set	Gene set	Inferred root
All	All	Between Lorantheae core clade and all other Loranthaceae (including Loranthinae and Ileostylinae; not used as rooting scenario for subsequent analyses)
All	All, excluding trnLLF	Between Lorantheae and all other Loranthaceae (= rooting scenario 2)
All	Nuclear ribosomal DNAs only	Between Lorantheae and all other Loranthaceae (= rooting scenario 2)
All	Chloroplast regions only	Between Lorantheae and all other Loranthaceae (= rooting scenario 2)
All	Chloroplast genes only	Between Lorantheae and all other Loranthaceae (= rooting scenario 2)
Reduced	All	Between <i>Nuytsia</i> and all other Loranthaceae (equals outgroup inferred root; = rooting scenario 1)

1

2



Table 3(on next page)

Results of the dating analyses using the reduced taxon data set and different rooting scenarios

Cells with same background colour refer to the same node. Abbreviations: u.b. = upper boundary, l.b. = lower boundary, of the 95%-highest-posterior-density interval; MRCA = most recent common ancestor (can be inclusive or exclusive). Medians closest to the arithmethic mean of all four scenarios (column 'Av.Medians') in bold, minimal age scenarios for each node (column 'Abs.min') highlighted by blue colour.

	Root	ing scenai	rio 1	Root	ing scena	rio 2	Roo	ting scena	rio 3		Scenario 4		Av.	Abs.		
Node	L.b.	Median	U.b.	L.b.	Median		L.b.	Median	U.b.	L.b.	Median	U.b.	Medians	min	Correspon	nds to
Loranthaceae crown	52.6	50.1	47.8	51.5	49.1	46.9	56.1	50.8	47.3	48.0	45.4	43.0	48.9	43.0	Earliest	Lutetian
Nuytsia root	52.6	50.1	47.8	50.4	48.1	45.9	47.4	41.6	34.2	48.0	45.4	43.0	46.3	34.2	Latest	Priabonian
Atkinsonia root	46.8	43.8	40.7	45.7	43.1	40.5	47.5	44.3	40.9	45.9	43.9	42.0	43.8	40.5	Early	Bartonian
Gaiadendron root	46.5	43.7	40.7	45.7	43.1	40.6	47.4	44.3	41.1	45.1	43.2	41.5	43.6	40.6	Early	Bartonian
Tristerix root	52.2	49.7	47.3	48.0	44.4	38.9	47.4	41.6	34.2	40.4	37.0	31.9	43.2	31.9	Latest	Priabonian
Tupeia root	49.7	47.2	44.8	48.0	44.4	38.9	56.1	50.8	47.3	42.2	39.1	32.7	45.4	32.7	Late	Bartonian
MRCA (aerial parasitic) New World														40.2		
taxa	52.2	49.7	47.3	48.7	46.8	44.9	50.8	48.5	46.2	42.8	41.4	40.2	46.6	-10.2	Mid	Lutetian
MRCA Desmaria-Ligaria	46.0	42.2	36.3	45.2	41.5	36.0	46.7	42.6	36.9	42.8	41.4	40.2	41.9	36.0	Mid	Priabonian
Notanthera + Elytrantheae root*	46.8	43.8	40.7	45.7	43.1	40.5	47.5	44.3	40.9		[N/A]		43.7	40.5	Early	Bartonian
MRCA Notanthera + Elytrantheae*	41.0	39.5	38.0	40.9	39.4	37.8	41.0	39.5	38.0	44.1	42.5	41.1	40.2	37.8	Latest	Bartonian
Notanthera + Psittacanthinae root*		[N/A]			[N/A]			[N/A]		42.2	40.9	39.7	40.9	39.7	Early	Bartonian
MRCA Notanthera + Psittacanthinae*	48.6	46.4	44.3	47.4	45.5	43.8	49.6	47.2	44.9	41.5	40.5	39.5	44.9	39.5	Early	Bartonian
Psittacanthinae root	47.1	45.0	43.0	46.2	44.4	42.6	47.9	45.5	43.4	41.5	40.5	39.5	43.8	39.5	Latest	Lutetian
Psittacanthinae crown	41.4	40.4	39.5	41.3	40.3	39.4	41.5	40.6	39.6	29.8	22.8	16.7	36.0	16.7	Mid	Bartonian
Elytrantheae root	41.0	39.5	38.0	40.9	39.4	37.8	41.0	39.5	38.0	42.6	41.2	39.6	39.9	37.8	Latest	Bartonian
Elytrantheae crown	38.5	33.4	26.7	38.2	33.1	26.6	38.5	33.5	27.0	35.1	27.2	20.2	31.8	20.2	Early	Chattian
Lorantheae root	49.7	47.2	44.8	51.5	49.1	46.9	51.4	49.1	46.8	42.6	41.2	39.6	46.7	39.6	Mid	Lutetian
Lorantheae crown	44.2	41.1	37.8	45.1	41.8	38.5	44.7	41.6	38.6	38.1	35.9	33.5	40.1	33.5	Earliest	Priabonian
Core Lorantheae crown	35.2	31.2	27.0	35.9	31.6	27.4	35.6	31.7	27.4	29.8	26.5	22.9	30.2	22.9	Early	Chattian

²

^{*} If topology is unconstrained, *Notanthera* is placed as sister to Elytrantheae ($BS_{ML} = ; PP =)$; in Scenario 4, *Notanthera* is constrained as sister of

Psittacanthinae (topological constraints derived from the tree shown in Su et al., 2015)



Table 4(on next page)

Estimated substitution rates (per million years) for each of the used genetic markers

Estimates are provided for all four tested topological hypotheses (rooting scenarios 1–3, and scenario 4 constraining the topology of Su et al. 2015).

1

	Rooting scenario 1	Rooting scenario 2	Rooting scenario 3	Scenario 4			
Genetic marker	Median ucld.mean						
18S rDNA	2.5*10-4	2.5*10-4	2.5*10-4	2.9*10-4			
25S rDNA	6.5*10-4	6.6*10-4	6.3*10-4	8.2*10-4			
matK	10.1*10-4	10.1*10-4	10.0*10-4	11.7*10-4			
trnLLFa	12.9*10-4	13.1*10-4	12.8*10-4	15.5*10-4			

^a Includes the *trn*L intron and downstream-located (5') *trn*L exon and *trn*L-*trn*F spacer



Table 5(on next page)

Ranking of the four tested topological configurations (three rooting scenarios, and scenario 4 constraining the topology of Su et al. 2015)

Ranking is based on marginal likelihood estimates (MLE) and Bayes factors (BF), calculated using two approaches, stepping-stone and path-sampling, implemented in Beast (Baele et al. 2012, 2013)



PeerJ

Rank	Scenario	Stepping-stor	Stepping-stone		Path-sampling	
		MLE	BF	MLE	BF	
1	Rooting sc. 3 <i>Tupeia</i> sister to rest	-29457.1		-29456.0		
2	Rooting sc. 1 <i>Nuytsia</i> sister to rest	-29461.0	7.87	-29460.0	8.08	
3	Scenario 4 (Su et al. 2015)	-29464.3	14.53	-29463.3	14.61	
4	Rooting sc. 2 (Lorantheae sister to rest)	-29466.3	18.54	-29465.7	19.43	

1